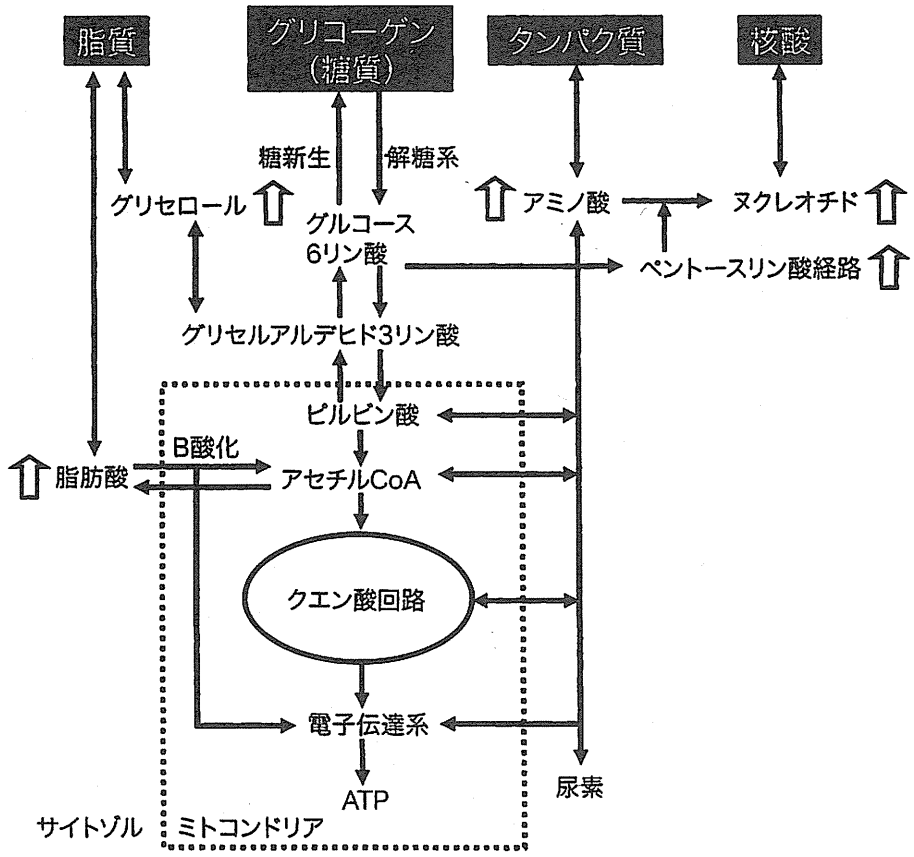

図2　代謝の概略とHCV感染が与える影響

生体内には核酸や蛋白質の他に，糖質，脂質，アミノ酸などの低分子が存在しており，これらの物質の多くは酵素などの代謝活動によって作りだされた代謝物質である．この図は糖質，脂質，アミノ酸，核酸が変化し，それらが相互に変換していることを示している．HCV感染に伴う代謝変化を矢印(上向きは増加)で示した[8]．HCV感染が中間代謝の複数の箇所に影響を及ぼしているのがわかるが，HCVがどこに直接作用しているかは不明である．

き，DNA配列の網羅的解析(ゲノミクス)や蛋白質の網羅的解析(プロテオミクス)が行われてきた．しかしながら，実際の細胞内ではホメオスタシスによりゲノムレベルでの変動が表現型に一致しないことも多い．その点で，代謝産物は表現型に最も近いため，表現型での変化が観察しやすいという特徴があり，代謝産物の網羅的解析(メタボロミクス)が注目されている．Roeらは，J6/JFHウイルスをHuh-7.5細胞に感染させ3日後にメタボローム解析を行ったところ，アミノ酸合成，RNA核酸合成，ペントースリン酸経路の亢進を認めた(図2)[8]．脂質代謝に関しては，HCV感染に伴い，グリセロリン脂質，スフィンゴ脂質，コレステロール，脂肪酸などが増加していた．グリセロリン脂質，スフィンゴ脂質，コレステロールはいずれも生体膜の主要脂質成分として知られており，その生活環の多くのステップで細胞の小胞体，ゴルジ体，細胞膜といった生体膜を利用しているHCVにとって好都合な状況となっていると考えられる．特に，スフィンゴ脂質，コレステロールは脂質ラフトの構成成分であることから，前述のようにHCVの感染，複製，粒子形成にも役立っているものと考えられる．筆者らも，JFHウイルスをHuh-7細胞に感染させ，

感染がすべての細胞に広がった9日目にメタボローム解析を行ったところ，TCA回路，プリン・ピリミジン合成系など蛋白核酸合成などは低下し，ATP，GTP，phosphocreatineなどのエネルギー供与体は減少し，一方解糖系は著明に亢進していた．これはウイルス増殖にエネルギーが消費され，解糖系を亢進させてエネルギーを補っている状態を示している可能性が考えられた．前述のRoeらの結果と異なるのは，JFHウイルスとJ6/JFHウイルスで増殖の形態が異なることなどによる可能性が考えられるが，詳細はさらなる検討が必要である．

2. HCVによる肝細胞の脂肪化

HCVによる肝細胞の脂肪化の機序はHCVコア遺伝子トランスジェニックマウスを用いた研究などで明らかになっている[9]．詳細は他項に譲るが，HCVコア蛋白は脂質合成系の転写因子sterol regulatory element binding protein-1の増加を介して，脂肪酸合成酵素の活性をあげて，脂肪酸合成を亢進させている．一方，ミトコンドリアに局在化したコア蛋白は脂肪酸のβ酸化を抑制し，脂肪酸の消費を低下させている．また，microsomal triglyceride transfer proteinを低下させるため，超低比重リポ蛋白(VLDL)分泌を抑制し，細胞外への脂肪酸の放出を抑制している．さらに，HCVが誘発するインスリン抵抗性による高インスリン血漿は脂肪細胞からの肝細胞への遊離脂肪酸の取り込みを増加させている．

脂質はリン脂質，コレステロール，脂肪酸，中性脂肪，コレステロールエステルに大別され，生体膜の主要成分として生体構造を司るとともに，エネルギー代謝の中心を担っており，生命維持のうえでも重要な役割を果たしている．食物として取り入れられた脂質は脂質代謝の流れに乗って全身の必要な臓器に移行する．この脂質輸送の中心を担っているのがリポ蛋白である．前述のようにHCV感染による肝脂肪化の原因のひとつとして，VLDL分泌低下が報告されている．一方，VLDLはHCVの感染性に必須と報告されており，筆者らはこれらの矛盾点を解明するためHCV感染に伴う肝細胞の脂肪化の分子メカニズムについて，リポ蛋白に注目し解析した．HCV感染後，培養上清中のVLDLの割合が増加し，低比重リポ蛋白(LDL)の割合が低下することをみいだし，その原因としてHCV感染細胞でのVLDL分解酵素であるHepatic lipaseの発現低下をみいだした．HCVの感染に伴う，肝細胞内での脂質の蓄積と培養上清中のVLDLの割合の増加は，ウイルスにとって合目的な作用といえる．

4 まとめ

以上のように，感染，複製，粒子形成，放出など，HCVはその生活環の多くのステップで宿主の脂質を巧みに利用していることがわかってきた．さらに，HCVは感染した細胞に脂質の蓄積という，HCV増殖に好都合な環境を作りだしているものと考えられる．また，感染細胞のメタボローム解析の結果，脂質代謝だけでなく，アミノ酸合成，RNA核酸合成，TCA回路，エネルギー産生系，糖新生・解糖系などに多彩な影響を与えている可能性が示された．このような解析はC型肝炎患者の病態の理解につながると期待できる．

文　献

1) Wakita T, Pietschmann T, Kato T et al : Production of infectious hepatitis C virus in tissue culture from a cloned viral genome. Nat Med 11 : 791–796, 2005

2) Aizaki H, Morikawa K, Fukasawa M et al : Critical role of virion-associated cholesterol and sphingolipid in hepatitis C virus infection. J Virol 82 : 5715–5724, 2008
3) Simons K, Ikonen E : Functional rafts in cell membranes. Nature 387 : 569–572, 1997
4) Lohmann V, Körner F, Koch J et al: Replication of subgenomic hepatitis C virus RNAs in a hepatoma cell line. Science 285 : 110–113, 1999
5) Aizaki H, Lee KJ, Sung VM et al : Characterization of the hepatitis C virus RNA replication complex associated with lipid rafts. Virology 324 : 450–461, 2004
6) Sakamoto H, Okamoto K, Aoki M et al : Host sphingolipid biosynthesis as a target for hepatitis C virus therapy. Nat Chem Biol 1 : 333–337, 2005
7) Sezaki H, Suzuki F, Akuta N et al : An open pilot study exploring the efficacy of fluvastatin, pegylated interferon and ribavirin in patients with hepatitis C virus genotype 1b in high viral loads. Intervirology 52 : 43–48, 2009
8) Roe B, Kensicki E, Mohney R et al : Metabolomic profile of hepatitis C virus-infected hepatocytes. PLoS One 6 : e23641, 2011
9) Moriya K, Yotsuyanagi H, Shintani Y et al : Hepatitis C virus core protein induces hepatic steatosis in transgenic mice. J Gen Virol 78 : 1527–1531, 1997
10) Aizaki H, Nagamori S, Aoki Y et al : The utilization of human hepatocyte in the study of hepatitis C virus; establishment of the efficient replication system of hepatitis C virus. Tiss Cult Res Commun 18 : 265–278, 1999

*　　*　　*

C型肝炎ウイルス研究の進歩
C型肝炎ウイルスの分子生物学

HCVの生活環における脂質の役割

Critical roles of lipids in the HCV life cycle

相崎英樹　鈴木哲朗　脇田隆字

Key words：HCV，生活環，脂質ラフト，脂肪滴

はじめに

C型肝炎ウイルス(HCV)には効率の良いウイルス培養系と実験用の感染小動物が存在しなかったため，HCVの基礎研究の妨げになり，抗ウイルス薬やワクチンの開発が遅れてきた．しかし，劇症肝炎患者から単離されたJFH-1株のゲノムRNAを肝癌細胞由来のHuh-7細胞に導入することにより，感染性ウイルス粒子を培養細胞で作製する技術が確立された[1]．これは，HCVの生活環(感染，翻訳，複製，ウイルス粒子形成，放出)をすべて再現可能な実験系であり，HCV研究を急速に加速させた．その研究成果から，HCVは宿主細胞の脂質代謝に影響を与えるだけでなく，宿主の脂質を巧みに利用して増殖していることがわかってきた．

本稿では，HCV生活環の各ステップにおける脂質の役割について解説したい．

1. 感染におけるHCV粒子の脂質の役割

エンベロープウイルスは小胞体，ゴルジ体，細胞膜などの細胞の生体膜を被って出芽するため，細胞の膜脂質はウイルス粒子形成に重要な役割を果たしているものと考えられる．しかし，HCV粒子に含まれる脂質成分については解析が進んでおらず，その生理学的役割も不明であった．そこで著者らは，培養細胞で産生させたHCV JFH-1粒子を，限外濾過，ショ糖密度勾配超遠心，ヘパリンアフィニティクロマトグラフィーを組み合わせて，培養上清から濃縮，粗精製し，このHCV粒子に含まれる脂質を生化学的に解析した．その結果，コレステロール/リン脂質モル比が細胞の膜分画に比べて有意に高値を示したことから，コレステロールに富んだ生体膜からの出芽，または粒子形成，分泌過程でのコレステロールとの会合の可能性が考えられた[2]．次にこのHCV粒子上の膜脂質がどのような役割を果たしているかを調べるため，HCV粒子表面をmethyl-B-cyclodextrin(B-CD)で処理してコレステロールを除去した後，感染させたところ，B-CDの用量依存的に感染性が低下し，B-CD処理した粒子にコレステロールを添加したところその感染性は回復した．また，生体膜の脂質の主要成分はコレステロールとスフィンゴ脂質であることから，スフィンゴ脂質の主要分子スフィンゴミエリンを加水分解するsphingomyelinase(SMase)でHCV粒子を処理したところ，感染性の低下を観察した．これらのことはHCV genotype 1bのエンベロープをもつシュードタイプウイルスやキメラウイ

Hideki Aizaki, Tetsuro Suzuki, Takaji Wakita: Department of Virology II, National Institute of Infectious Diseases
国立感染症研究所 ウイルス二部

0047-1852/11/¥60/頁/JCOPY

ルスでも確認できた．以上から，ウイルス粒子表面のコレステロールとスフィンゴ脂質はウイルスの遺伝子型によらず感染に重要な役割を果たしていることが示された．次に，HCV粒子上のコレステロールまたスフィンゴ脂質が感染過程のどのステップに関与するのかを解析した．あらかじめB-CD処理またはSMase処理を行ったHCV粒子の宿主細胞への吸着性は未処理ウイルスと同等であったのに対し，吸着後の細胞内への取り込みは，これらの前処理を施したHCVで顕著な低下が認められた．レセプタータンパク分子とともに標的細胞内へウイルスが侵入する過程に粒子コレステロール，スフィンゴ脂質が関与する可能性が示された．

細胞膜上のスフィンゴ脂質とコレステロールに富んだ微小領域は脂質ラフトと呼ばれている[3]．この脂質ラフトは，膜表面上をイカダのように漂いながら，ラフト同士が結合して島状のものになったり，小胞を形成したりと，ダイナミックに変化しながら，ラフトに結合するタンパク質の濃縮や細胞内輸送，シグナルトランスダクション，脂質代謝を担っていると考えられている．HCVエンベロープは脂質ラフト上で機能的な形態，すなわち感染性を示す可能性が考えられた．また，脂質ラフトはインフルエンザウイルスの集合・出芽，ヒト免疫不全ウイルスの集合・出芽や侵入，エボラウイルスの集合，コクサッキーウイルスA9の侵入，HTLV-1の膜融合や集合，マウス白血病ウイルスの侵入，麻疹ウイルスの集合，センダイウイルスの集合，RSウイルスの集合，マーブルグウイルス，ロタウイルスの集合，ヒト単純ヘルペスウイルスの集合や侵入，エコーウイルス11の侵入，などの多くのウイルスの侵入や粒子形成に重要な役割を果たしていることが報告されている．

2. 感染における細胞膜(形質膜)の脂質の役割

ウイルスの細胞表面への吸着および侵入は，ウイルス感染の最も初めのステップである．著者らはこの感染の過程において細胞表面の脂質の役割について解析した[2]．細胞表面をB-CDで処理してコレステロールを除去した後，HCVを感染させたところ，B-CDの用量依存的に感染性が低下した．また，細胞表面をSMaseで処理することにより感染性の低下を観察した．Kapadiaらは，細胞表面のコレステロールはCD81の細胞表面での安定性にかかわると報告しており，Voissetらはスフィンゴミエリンの加水分解産物であるceramideがCD81の細胞内取り込みを亢進させると説明している．以上の結果から，細胞表面のコレステロールやスフィンゴ脂質がHCV感染において重要な役割を果たしているものと考えられる．

3. ウイルスゲノム複製における脂質の役割

1999年，ドイツのグループは，本来HCVゲノムの中でウイルス粒子を形成する構造タンパク質領域を薬剤耐性遺伝子に置き換え，その下流に，より強力にHCVゲノムの内部から翻訳させる働きを有するencepharomyocarditis virus(EMCV)のIRESを挿入したRNAレプリコンを作製した[4]．このRNAをトランスフェクトした細胞を薬剤存在下で培養することで，自律複製するために必要な適応変異を獲得したHCVゲノムと，更にこのHCV遺伝子が複製しうる細胞を選択することを可能にした．著者らはこのレプリコン細胞を用いて，アクチノマイシンD処理して細胞内のDNA依存性RNAポリメラーゼを抑えたうえで，5-bromouridine 5′-triphosphate(BrUTP)を細胞に導入し，免疫組織染色で観察した[5]．BrUTPが取り込まれた新規に合成されたHCV RNAはレプリコン細胞の核周辺の細胞質に斑点状の構造物として認められ，これらはNSタンパクと共局在した．レプリコン細胞を電子顕微鏡で観察すると'membranous web'と呼ばれる小胞様構造物が認められることが報告されており[6]，HCVのすべての構造，非構造タンパクを強制発現させても同様の膜変化が生じることが知られている．以上のことから，HCVの複製複合体は感染細胞のmembranous webに存在しているものと考えら

れている.

次に，生化学的手法を用いて，複製活性を維持したままのHCV複製複合体を粗精製し解析した[7]．細胞のlysateを非イオン性界面活性剤で処理した後，分画したところ，HCV RNAとNSタンパクの大部分は界面活性剤不溶性膜画分(DRM)に残った．それぞれの画分に標識化合物(CTP)を加え，この取り込みを指標にしたHCV RNA複製活性測定を行ったところ，活性はDRMにのみ検出された．以上のことから，このDRMに複製活性を保持したHCV複製複合体が存在することが判明したことから，HCV複製複合体が脂質ラフト上で形成される可能性が示唆された．脂質ラフトはコレステロールとスフィンゴ脂質からなると考えられている[3]．そこで，HMG-CoAレダクターゼ阻害剤のロバスタチンでレプリコン細胞内のコレステロール合成を抑制したところHCV RNA複製効率も落ちたことから，脂質ラフトがHCV複製複合体と結合し，HCV複製において重要な役割を果たしている可能性が示唆された．また，各種スフィンゴ脂質合成阻害剤が脂質ラフト形成を抑制することで，ウイルス複製を抑えるという報告があり，脂質ラフトの存在する膜上で複製が起こるという仮説が支持された[8]．

HCVNSタンパクはERで合成され，NS4Bは膜に，NS5Aはその5末端で，NS5Bはその3末端で膜にアンカーし，HCVNSタンパク同士で結合する．また，著者らは細胞内膜タンパク質の一つで，細胞内膜輸送にかかわっていると考えられているthe human homologue of the 33-kDa vesicle-associated membrane protein-associated protein(VAP-A)はそのN末端でNS5Bと，中央部のコイルドコイル領域でNS5Aと結合することを見いだしている[9]．NS5Aは脂質ラフトと弱く結合し，NS4Bは強く結合する．以上から，NS4Bが中心となって，hVAP-33やNS5A，5Bとともに，ほかのNSタンパクを脂質ラフト上に誘導・固定する役割を担っているものと思われる．更に，脂質ラフトはNSタンパクを集積させ，結合体を形成させるだけでなく，小胞構造をとり，膜に包まれたHCV複製の場を提供する役割があるものと想定されている[7]．HCV複製複合体は脂質ラフトを含む膜小胞構造内に存在し，内部に存在するHCV RNAやNSタンパクは外部からのRNA分解酵素やプロテアーゼに対して保護されているものと考えられた．

4. HCV粒子形成における脂肪滴の役割

HCV粒子の形成，分泌過程の解析もウイルス培養系の開発により可能となり，脂肪滴の役割が注目されている．Miyanariらはウイルス感染細胞内で脂肪滴をコアタンパク質が被い，更にそのコアタンパクをNS5Aタンパクが被っていることを発見した[10]．NS5AタンパクはER膜上で形成され，脂肪滴上に移行し，そこに存在するコアタンパクと結合していた．コアとNS5Aタンパクが結合できない変異をウイルスゲノムに導入すると，感染性ウイルス粒子の形成がなくなったことから，感染性ウイルス粒子の形成には脂肪滴上でのコアとNS5Aタンパク質の結合が重要であると考えられた．Masakiらは，NS5Aのdomain IIIの変異体ではコアタンパクと結合できなくなること，またこの変異によってNS5Aタンパクは脂肪滴周辺膜に局在できなくなること，を見いだした[11]．更に，新たに合成されたHCVゲノムはNS5Aのdomain I部位と結合し，NS5Aのdomain IIIとコアタンパクとが会合することで，HCVゲノムへのコアの会合が起こり，ヌクレオカプシドが形成される可能性を見いだした．最近，ERに存在し脂肪滴産生に寄与しているdiacylglycerol acyltansferase-1(DGAT1)がコアタンパクと結合し，コアタンパクの脂肪滴への輸送を担っていることが報告された[12]．翻訳されたコアタンパクC末端の膜貫通領域はER膜に貫通しているが，DGAT1に結合したコアタンパクは膜貫通領域がER膜内でsignal peptide peptidase(SPP)に切断されて成熟コアタンパクになると考えられている．膜貫通領域がこの切断により短くなり脂肪滴の1枚の膜上に自由に移動できるようになり，更にコアタンパクの疎水性領域が脂質に親和性があり脂肪滴上に蓄積するものと考えら

れる[13].

5. HCV粒子形成におけるリポタンパクの役割

脂肪滴周辺で形成されたHCV粒子は，リポタンパク形成や分泌を抑制すると感染性HCV粒子放出も減少することから，HCVは超低比重リポタンパク(VLDL)分泌系を利用している可能性が考えられている[14]．HCVゲノムを囲むようにヌクレオカプシドが形成され，その周りにヘテロダイマーを形成したE1とE2タンパクが覆っている．最近，更にこの粒子がVLDLや低比重リポタンパク(LDL)に包まれていることを示す報告が集積してきている．E1とE2にはHDL，LDL，VLDLと結合する性質があり，リポタンパクに含まれるapolipoprotein E(ApoE)，ApoB，ApoC1などが感染性に重要ということが報告されている．

おわりに

これまでの研究から，①ウイルス粒子膜は脂質に富んでおり感染に重要，②細胞の細胞膜の脂質も感染に重要，③細胞の生体膜脂質はウイルスゲノム複製に重要，④脂肪滴が粒子形成に重要，⑤ウイルス粒子はリポタンパク分泌系を利用して放出され，⑥ウイルス粒子の被るリポタンパクは感染性に重要など，HCVはその生活環の多くのステップに脂質を必要としていることがわかってきた．したがって，細胞内脂質代謝をコントロールすることでウイルス増殖を抑えられる可能性がある．実際に，C型肝炎患者のインターフェンロン(IFN)での治療の際にコレステロール値を下げる効果のあるスタチン製剤を併用させるとHCV治療効果を高めるという報告もある[15]．

HCVはゲノム配列が多様で，大変変異しやすいウイルスであり，IFNやリバビリンなどの薬剤に対しても耐性をもつウイルスが出現しやすいことが知られている．新たな抗HCV薬として，ウイルスプロテアーゼやポリメラーゼなどのウイルス複製に関与する酵素を標的とした薬剤の開発研究が盛んに行われている．HIVと同様にこれらの薬剤についてもHCVは耐性変異を獲得することが報告されている．本稿で報告した宿主のコレステロール産生系やスフィンゴ脂質の産生系など，ウイルス生活環に関与する宿主因子を標的とし，感染した細胞側の働きを抑えてウイルス増殖を抑制する抗HCV薬の開発は耐性ウイルスが出現しにくい薬剤につながる期待がある．

文献

1) Wakita T, et al: Production of infectious hepatitis C virus in tissue culture from a cloned viral genome. Nat Med 11: 791-796, 2005.
2) Aizaki H, et al: Critical role of virion-associated cholesterol and sphingolipid in hepatitis C virus infection. J Virol 82: 5715-5724, 2008.
3) Simons K, Ikonen E: Functional rafts in cell membranes. Nature 387: 569-572, 1997.
4) Lohmann V, et al: Replication of subgenomic hepatitis C virus RNAs in a hepatoma cell line. Science 285: 110-113, 1999.
5) Shi ST, et al: Hepatitis C virus RNA replication occurs on a detergent-resistant membrane that cofractionates with caveolin-2. J Virol 77: 4160-4168, 2003.
6) Egger D, et al: Expression of hepatitis C virus proteins induces distinct membrane alterations including a candidate viral replication complex. J Virol 76: 5974-5984, 2002.
7) Aizaki H, et al: Characterization of the hepatitis C virus RNA replication complex associated with lipid rafts. Virology 324: 450-461, 2004.
8) Sakamoto H, et al: Host sphingolipid biosynthesis as a target for hepatitis C virus therapy. Nat Chem Biol 1: 333-337, 2005.
9) Gao L, et al: Interactions between viral nonstructural proteins and host protein hVAP-33 mediate the formation of hepatitis C virus RNA replication complex on lipid raft. J Virol 78: 3480-3488, 2004.
10) Miyanari Y, et al: The lipid droplet is an important organelle for hepatitis C virus production. Nat

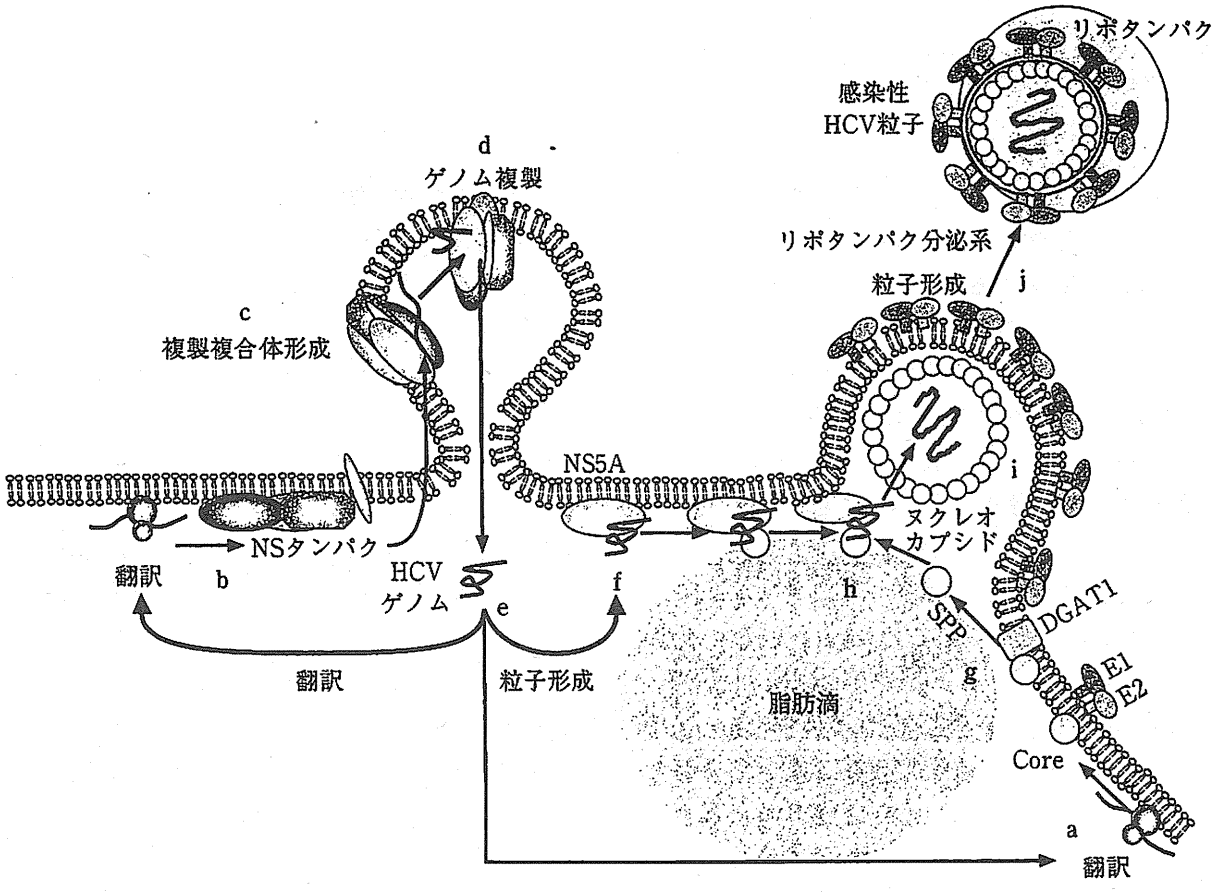

図1 HCV粒子形成モデル

HCVがレセプターを介して肝細胞に感染し，粒子よりウイルスRNAが放出され，これがメッセンジャーRNAとして働き，このRNAの5′非翻訳領域に存在するIRESから翻訳が開始され大きな前駆体タンパクが合成される．この前駆体タンパクは，細胞のシグナラーゼによってウイルス粒子を形成する構造タンパクであるコアタンパクと2つのエンベロープタンパクE1，E2がプロセスされる(a)．また，ウイルス自身がコードするプロテアーゼによって，プロテアーゼ，ヘリカーゼ，RNA依存性RNAポリメラーゼなどウイルスの複製に必須な非構造タンパクがプロセスされる(b)．ウイルスにコードされた酵素や宿主因子によって複製複合体が形成され(c)，ゲノムRNAからマイナス鎖RNAが転写され，これを基にしてプラス鎖RNAが複製され(d)，新生されたHCV RNAは翻訳に使われるものと粒子形成に用いられるものに分かれる(e)．粒子形成に用いられるHCV RNAはNS5Aタンパクと結合し，脂肪滴周辺膜へと運ばれる(f)が，そのNS5Aの移行メカニズムはわかっていない．一方，翻訳されたコアタンパクはDGAT1に結合し，膜貫通領域がER膜内でSPPに切断されて成熟コアタンパクになり(g)，脂肪滴に移行する．脂肪滴上のコアとNS5Aタンパクは結合することで(h)，ウイルスRNAがコアタンパクと結合してヌクレオカプシドを形成し(i)，粒子を形成し，VLDL分泌系を利用して，放出されるものと考えられている(j)．

Cell Biol 9: 1089–1097, 2007.
11) Masaki T, et al: Interaction of hepatitis C virus nonstructural protein 5A with core protein is critical for the production of infectious virus particles. J Virol 82: 7964–7976, 2008.
12) Herker E, et al: Efficient hepatitis C virus particle formation requires diacylglycerol acyltransferase–1. Nat Med 16: 1295–1298, 2010.
13) Okamoto K, et al: Intramembrane processing by signal peptide peptidase regulates the membrane localization of hepatitis C virus core protein and viral propagation. J Virol 82: 8349–8361, 2008.
14) Huang H, et al: Hepatitis C virus production by human hepatocytes dependent on assembly and secretion of very low–density lipoproteins. Proc Natl Acad Sci USA 104: 5848–5853, 2007.
15) Sezaki H, et al: An open pilot study exploring the efficacy of fluvastatin, pegylated interferon and ribavirin in patients with hepatitis C virus genotype 1b in high viral loads. Intervirology 52: 43–48, 2009.

Visualization and Measurement of ATP Levels in Living Cells Replicating Hepatitis C Virus Genome RNA

Tomomi Ando[1,2], Hiromi Imamura[3], Ryosuke Suzuki[1], Hideki Aizaki[1], Toshiki Watanabe[2], Takaji Wakita[1], Tetsuro Suzuki[4]*

1 Department of Virology II, National Institute of Infectious Diseases, Tokyo, Japan, 2 Graduate School of Frontier Sciences, The University of Tokyo, Tokyo, Japan, 3 The Hakubi Center and Graduate School of Biostudies, Kyoto University, Kyoto, Japan, 4 Hamamatsu University School of Medicine, Department of Infectious Diseases, Hamamatsu, Japan

Abstract

Adenosine 5′-triphosphate (ATP) is the primary energy currency of all living organisms and participates in a variety of cellular processes. Although ATP requirements during viral lifecycles have been examined in a number of studies, a method by which ATP production can be monitored in real-time, and by which ATP can be quantified in individual cells and subcellular compartments, is lacking, thereby hindering studies aimed at elucidating the precise mechanisms by which viral replication energized by ATP is controlled. In this study, we investigated the fluctuation and distribution of ATP in cells during RNA replication of the hepatitis C virus (HCV), a member of the *Flaviviridae* family. We demonstrated that cells involved in viral RNA replication actively consumed ATP, thereby reducing cytoplasmic ATP levels. Subsequently, a method to measure ATP levels at putative subcellular sites of HCV RNA replication in living cells was developed by introducing a recently-established Förster resonance energy transfer (FRET)-based ATP indicator, called ATeam, into the NS5A coding region of the HCV replicon. Using this method, we were able to observe the formation of ATP-enriched dot-like structures, which co-localize with non-structural viral proteins, within the cytoplasm of HCV-replicating cells but not in non-replicating cells. The obtained FRET signals allowed us to estimate ATP concentrations within HCV replicating cells as ~5 mM at possible replicating sites and ~1 mM at peripheral sites that did not appear to be involved in HCV replication. In contrast, cytoplasmic ATP levels in non-replicating Huh-7 cells were estimated as ~2 mM. To our knowledge, this is the first study to demonstrate changes in ATP concentration within cells during replication of the HCV genome and increased ATP levels at distinct sites within replicating cells. ATeam may be a powerful tool for the study of energy metabolism during replication of the viral genome.

Citation: Ando T, Imamura H, Suzuki R, Aizaki H, Watanabe T, et al. (2012) Visualization and Measurement of ATP Levels in Living Cells Replicating Hepatitis C Virus Genome RNA. PLoS Pathog 8(3): e1002561. doi:10.1371/journal.ppat.1002561

Editor: Andrea Gamarnik, Fundación Instituto Leloir-CONICET, Argentina

Received August 22, 2011; **Accepted** January 18, 2012; **Published** March 1, 2012

Funding: This work was supported by a grant-in-aid for Scientific Research from the Japan Society for the Promotion of Science, from the Ministry of Health, Labour and Welfare of Japan and from the Ministry of Education, Culture, Sports, Science and Technology of Japan. T.A. is a research fellow of the Japan Society for the Promotion of Science. The funders had no role in study design, data collection and analysis, decision to publish, or preparation of the manuscript.

Competing Interests: The authors have declared that no competing interests exist.

* E-mail: tesuzuki@hama-med.ac.jp

Introduction

Adenosine 5′-triphosphate (ATP) is the major energy currency of cells and is involved in a variety of cellular processes, including the virus life cycle, in which ATP-dependent reactions essential for virus multiplication are catalyzed by viral-encoded enzymes or complexes consisting of viral and host-cell proteins [1]. However, the lack of a real-time monitoring system for ATP has hindered studies aimed at elucidating the mechanisms by which cellular processes are controlled through ATP. A method for measuring ATP levels in individual living cells has recently been developed using a genetically-encoded FRET-based indicator for ATP, called ATeam, which employs the epsilon subunit of a bacterial F_0F_1-ATPase [2]. The epsilon subunit has several theoretical advantages for use as an ATP indicator; i) small size (14 kDa), ii) high specific binding to ATP, iii) ATP binding induces a global conformational change and iv) ATP hydrolysis does not occur following binding [3–5]. The affinity of ATeam for ATP can be adjusted by changing various amino acid residues in the ATP-binding domain within the subunit. ATeam has enabled researchers to examine the subcellular compartmentation of ATP as well as time-dependent changes in cellular ATP levels under various physiological conditions. For example, the ATeam-based method has been used to demonstrate that ATP levels within the mitochondrial matrix are lower than those in the cytoplasm and the nucleus [2].

Hepatitis C virus (HCV) infects 2–3% of the world population and is a major cause of chronic hepatitis, liver cirrhosis and hepatocellular carcinoma [6–8]. HCV possesses a positive-strand RNA genome and belongs to the family *Flaviviridae*. A precursor polyprotein of ~3000 amino acids is post- or co-translationally processed by both viral and host proteases into at least ten viral products. The nonstructural (NS) proteins NS3, NS4A, NS4B, NS5A and NS5B are necessary and sufficient for autonomous HCV RNA replication. These proteins form a membrane-associated replication complex (RC), in which NS5B is the RNA-dependent RNA polymerase (RdRp) responsible for copying the RNA genome of the virus during replication [9,10]. NS3, in addition to its protease activity, functions as a viral helicase capable of separating duplex RNA and DNA in reactions fuelled

Author Summary

ATP is the major energy currency of living cells. Replication of the virus genome is a physiological mechanism that is known to require energy for operations such as the synthesis of DNA or RNA and their unwinding. However, it has been difficult to comprehend how the ATP level is regulated inside single living cells where the virus replicates, since average ATP values in cell extracts have only been estimated using existing methods for ATP measurement. ATeam, which was established in 2009, is a genetically-encoded Förster resonance energy transfer (FRET)-based indicator for ATP that is composed of a small bacterial protein that specifically binds ATP sandwiched between two fluorescent proteins. In this study, by applying ATeam to the subgenomic replicon system, we have developed a method to monitor ATP at putative subcellular sites of RNA replication of the hepatitis C virus (HCV), a major human pathogen associated with liver disease, in living cells. We show here, for the first time, changes in ATP concentrations at distinct sites within cells undergoing HCV RNA replication. ATeam might open the door to understanding how regulation of ATP can affect the lifecycles of pathogens.

by ATP hydrolysis [11,12]. Consistent with other positive-strand RNA viruses, replication of HCV genomic RNA is believed to occur in membrane-bound vesicles. NS3-NS5B proteins, together with several host-cell proteins, form a membrane-associated RC. The HCV RC is localized to distinct dot-like structures within the cytoplasm of HCV replicating cells and can be detected in detergent-resistant membrane structures [13].

In this study, we first used capillary electrophoresis-time-of-flight mass spectrometry (CE-TOF MS) and the original ATeam method to determine ATP levels in cells infected with HCV or replicating HCV RNA. Using these methods, together with an ATP consumption assay, we demonstrated that ATP is actively consumed in cells in which viral RNA replicates, leading to a reduction in cytoplasmic ATP compared to parental cells. To further understand the fluctuation and distribution of ATP in HCV replicating cells, we developed a system to monitor ATP at putative subcellular sites of HCV RNA replication in single living cells by applying ATeam technology to the subgenomic replicon system. Our results show that, in viral RNA-replicating cells, ATP levels are elevated at distinct dot-like structures that may play a supportive role in HCV RNA replication, while cytoplasmic levels of ATP decrease.

Results

The concentration of ATP is reduced in HCV-infected cells

As a first approach, the concentration of adenosine nucleotides within HCV-infected and non-infected cells was quantified by CE-TOF MS analysis. ATP levels were approximately 7- and 50-fold higher, respectively, than the levels of ADP and AMP in non-infected Huh-7 cells (Figure 1A). At 9 days post-infection with HCV particles produced from a wild-type JFH-1 isolate [14], the intracellular levels of ATP, ADP and AMP were significantly (52–59%) lower than those in naïve Huh-7 cells (Figure 1A). ATP/ADP and ATP/AMP ratios were comparable among HCV-infected and non-infected cells (Figure 1B). A similar result was obtained using JFH-1/4-5 cells that harbor a HCV subgenomic replicon (SGR) RNA derived from the JFH-1 isolate [15]; the intracellular ATP level of JFH-1/4-5 cells was lower than that of parental Huh-7 cells (Figure S1). These findings are basically consistent with a recent report that phosphorylation-mediated activation of AMP-activated protein kinase is inhibited in cells undergoing HCV genome replication, and that ATP/ADP ratios are similar among cells that do and do not demonstrate HCV replication [16,17].

Measurement of ATP levels in HCV-replicating cells using ATeam

To visualize ATP levels in living cells undergoing HCV genomic replication, one of the ATeam indicators, AT1.03^{YEMK}, which has a high affinity for ATP, was introduced into HCV replicon cells carrying SGR RNA or into parental Huh-7 cells and was imaged using confocal fluorescence microscopy. Consistent with previous observations in HeLa cells [2], this ATP indicator was distributed throughout the cytoplasm. FRET signals (Venus/

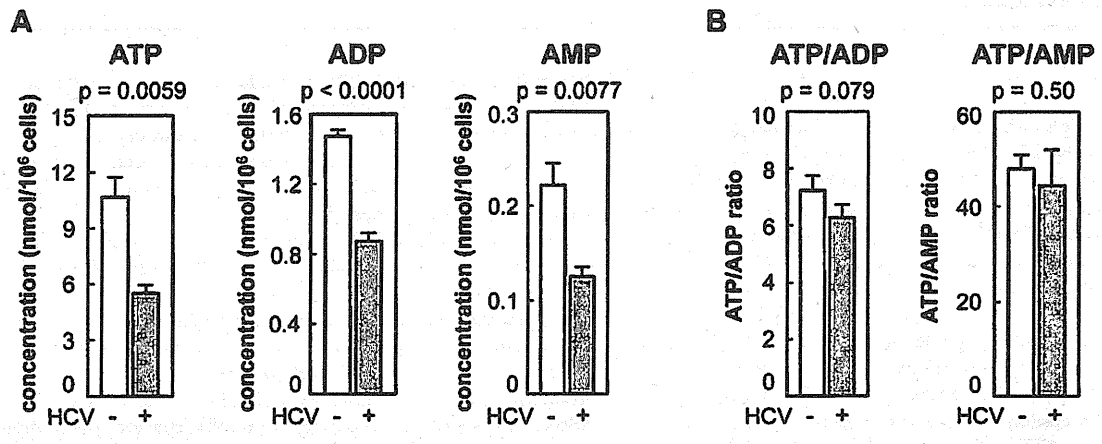

Figure 1. Levels of adenosine nucleotides in HCV-infected and non-infected Huh-7 cells determined by CE-TOF MS. (A) ATP levels were reduced in HCV-infected cells. ATP, ADP, and AMP metabolites in Huh-7 cells with (gray bars) and without (open bars) HCV infection were measured by CE-TOFMS. (B) Ratios of ATP/ADP and ATP/AMP were calculated from the results depicted in (A). All data are presented as means and standard deviation (SD) values for three independent samples. Statistical differences between HCV-infected and non-infected cells were evaluated using Student's *t*-test.
doi:10.1371/journal.ppat.1002561.g001

CFP fluorescence emission ratios), which reflect ATP levels in living cells, were calculated from the fluorescent images of CFP and Venus, a variant of YFP that is resistant to intracellular pH [18], within the cytoplasm of individual cells. Each independent measurement was plotted as indicated in Figure 2. Uniform Venus/CFP ratios were observed in Huh-7 cells. These ratios were reduced dramatically following combined treatment with 2-deoxyglucose (2DG) and Oligomycin A (OliA), which inhibit glycolysis and the oxidative phosphorylation of ADP to ATP, respectively [2]. When AT1.03^{YEMK} was expressed in the HCV replicon-harboring cells JFH-1/4-1, JFH-1/4-5 (genotype 2a) and NK5.1/0-9 (genotype 1b) [15], Venus/CFP ratios were significantly lower than those seen in parental Huh-7 cells. This result is consistent with the mass spectrometry results shown in Figures 1A and S1. Venus/CFP ratios were more variable in the replicon-carrying cells compared to Huh-7 cells. It is possible that ATP levels in the replicon cells correlate with viral replication levels, which may vary among the cells tested.

The consumption of ATP is increased in HCV-replicating cells

It has been reported that ATP is involved in different steps in the course of HCV replication such as in the initiation of RNA synthesis by NS5B RdRp [9]. NS3 unwinds RNA in an ATP-dependent manner and may be involved in viral replication [11,19,20]. NS4A has been shown to enhance the ability of the NS3 helicase to bind RNA in the presence of ATP [21]. In addition, ATP is generally used as a material in RNA synthesis. Together with the above results (Figures 1 and 2), one may hypothesize that active consumption of ATP in cells where HCV RNA replicates efficiently results in lower levels of cytoplasmic ATP compared to cells in the absence of the viral RNA. To study the influence of HCV RNA replication on the consumption of ATP in cells, we used permeabilized HCV replicon cells [13,22].

Following the addition of ATP to permeabilized cells, reduced ATP levels were detected using a luciferase-based assay (see Materials and Methods for details). Fifteen minutes after the addition of ATP, ATP levels in permeabilized replicon-carrying cells (JFH-1/4-1, JFH-1/4-5 and NK5.1/0-9) were reduced by 82–95%, and this reduction was greater than that observed in control Huh-7 cells (47%)(Figure 3). When the replication of HCV RNA was inhibited by pre-treatment of the cells with the cytidine analogue inhibitor of HCV NS5B polymerase, PSI-6130 [23,24], for 3 days, the reduction in ATP levels in the replicon cells was comparable to that of Huh-7 cells. A decrease in ATP reduction in the replicon cells was observed even following a 15-min treatment with the inhibitor. An effect of inhibition of viral replication on cytoplasmic ATP levels in replicon cells was also observed by ATeam-based analysis of Venus/CFP ratios following inhibition of replication by IFN-alpha (Figure S2). These results suggest that ATP is actively consumed during viral replication in HCV replicon cells, leading to decreased levels of ATP in the cytoplasm.

Development of a system to monitor ATP levels at putative subcellular sites of HCV replication in single living cells

Moradpour et al. have established functional HCV replicons that have either an epitope tag or the coding sequence for a green fluorescent protein (GFP) inserted in frame close to the C-terminus of NS5A, which they used to demonstrate incorporation of the NS5A-GFP fusion protein into the viral RC [25]. To further investigate intracellular changes in ATP during HCV replication, we generated HCV JFH-1-based subgenomic replicons harboring an ATeam insertion in the 3′ region of NS5A (SGR-ATeam), as

	No. cells	Venus/CFP ratio mean	Venus/CFP ratio SD	p-value vs Huh-7
Huh-7	19	2.08	0.090	
Huh-7 + 2DG, OliA	13	0.66	0.074	< $1x10^{-29}$
JFH-1/4-1	18	1.79	0.14	< $1x10^{-7}$
JFH-1/4-5	18	1.77	0.28	0.00019
NK5.1/0-9	19	1.66	0.30	< $1x10^{-5}$

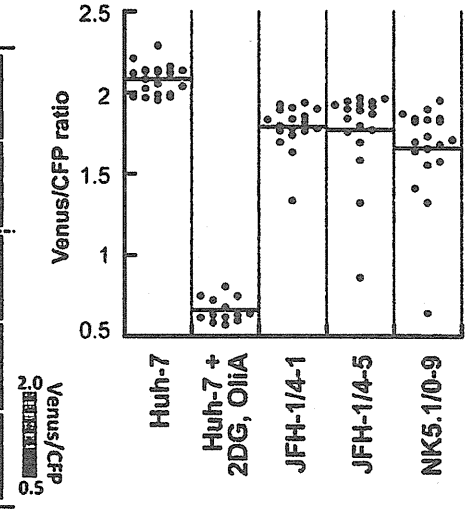

Figure 2. ATP fluctuations within the cytoplasm of HCV replicating cells analyzed using the original ATeam. Huh-7 cells carrying a HCV subgenomic replicon, JFH-1/4-1, JFH-1/4-5 (genotype 2a), and NK5.1/0-9 (genotype 1b) and parental Huh-7 cells were transfected with an ATP probe, AT1.03^{YEMK}. Forty-eight hours after transfection, the Venus/CFP emission ratio in the cytoplasm of each cell was calculated from fluorescent images acquired with a confocal microscope FV1000 (Olympus). Huh-7 cells treated with 10 mM 2-DG and 10 μg/ml OliA for 20 min were used as a negative control. Data are presented as means and standard deviation values (SD) for each cell. Statistical differences among Huh-7 cells were evaluated using Student's *t*-test. Pseudocolored images of Venus channel/CFP channel ratios of representative cells and a pseudocolor scale are shown. In the graph on the right, each plot indicates the Venus/CFP ratio of each cell. The horizontal lines in the center represent the mean values for each group.
doi:10.1371/journal.ppat.1002561.g002

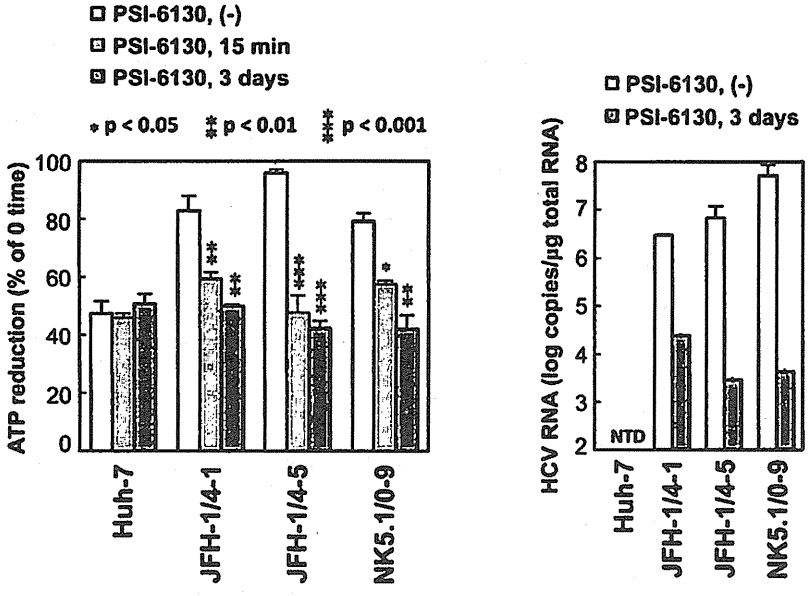

Figure 3. ATP consumption in cells replicating HCV RNA. (Left) The indicated cell lines were pretreated with 10 μM PSI-6130 for 3 days or were cultured in the absence of the drug, followed by trypsinization and permeabilization. ATP-containing reaction buffer plus 10 μM PSI-6130 was added to some of the non-pre-treated cells (PSI-6130, 15 min; light gray bars). ATP-containing PSI-6130-free reaction buffer was added to the rest of the non pre-treated cells (PSI-6130, (−); white bars) and to the pre-treated cells (PSI-6130, 3 days; dark gray bars). After 15 min incubation, ATP levels in cell lysates were measured using a luciferase-based assay. ATP reduction compared to ATP levels at the 0-time point was calculated. The mean values of three independent samples with SD are displayed. Statistical differences between cells treated with and without treatment with PSI-6130 were evaluated using Student's *t*-test. (Right) HCV RNA titers in cells corresponding to the left panel were determined using real-time quantitative RT-PCR. Data are presented as means and SD for three independent samples. NTD indicates not detected.
doi:10.1371/journal.ppat.1002561.g003

well as plasmids expressing NS5A-ATeam fusion proteins (NS5A-ATeam)(Figures 4A and 4C).

We first tested whether NS5A-ATeam fusion proteins can be used to monitor ATP levels over a range of concentrations in living cells. The Venus/CFP ratios in individual cells expressing NS5A fused either with AT1.03^{YEMK} (Kd = 1.2 mM at 37°C [2]) or with a relatively lower affinity version, AT1.03 (Kd = 3.3 mM at 37°C [2]) were measured. As shown in Figure 4B, differences in the Venus/CFP ratios of NS5A- AT1.03^{YEMK} and NS5A-AT1.03 were similar to those of AT1.03^{YEMK} and AT1.03, although average ratios were lower for NS5A- AT1.03^{YEMK} and NS5A-AT1.03 compared to AT1.03^{YEMK} and AT1.03. In the presence of 2DG and OliA, Venus/CFP ratios of NS5A-AT1.03^{YEMK} were markedly reduced to levels that were comparable to those of AT1.03^{RK}, an inactive mutant with R122K/R126K substitutions [2]. These results demonstrate that NS5A-ATeams can function as ATP indicators, although their dynamic ranges of Venus/CFP ratios are slightly smaller than those of the original, non-fused ATeams.

We next investigated whether the SGR-ATeam could initiate and sustain transient replication of HCV RNA in cells. A RNA polymerase I (Pol I)-derived plasmid, which carries SGR/luc-AT1.03 containing a luciferase reporter gene ([26]; Figure 4C), or its replication-defective mutant were transfected into Huh-7 cells and levels of viral replication were determined by measuring luciferase activity at various time intervals over a five day period (Figure 4D). Although replication of SGR/luc-AT1.03 was delayed compared with parental SGR/luc, the luciferase activity expressed from SGR/luc-AT1.03 rose to approximately a thousand-fold higher than that expressed from SGR/luc-GND-AT1.03 at five days post-transfection. It appears that SGR-AT1.03, which does not carry the luciferase gene, replicated more efficiently than SGR/luc-AT1.03, as determined by Western blotting of the HCV NS5B protein within cells four days post-transfection (Figure 4E). As indicated in Figure 4F, an abundant protein of the same size as that expected for the NS5A-ATeam fusion protein was observed in cells expressing either NS5A-AT1.03 or SGR-AT1.03, indicating that the NS5A-ATeam fusion protein is stable and is not cleaved during HCV replication. Thus, we concluded that the modified replicon constructs in which the ATeam is incorporated into the NS5A region are functional and remain capable of efficient transient replication of HCV RNA.

Visualization of ATP levels and distinctive features of ATP distribution in cells replicating ATeam-tagged SGR

This SGR-ATeam system that was established to analyze cellular ATP levels was used in living HCV RNA-replicating cells in which membrane-associated RCs are formed through the interaction of viral proteins, including NS5A, and cellular proteins. We compared the subcellular distribution of fluorescent signals expressed from NS5A-ATeams and SGR-ATeams using emission-scanning confocal fluorescence microscopy with a Zeiss META detector. NS5A-AT1.03 and NS5A-AT1.03^{YEMK} were diffusely distributed throughout the cytoplasm (Figure 5A; upper panels). Venus/CFP ratios of NS5A-ATeam constructs were almost constant throughout the cytoplasm (Figure 5A; lower). As expected, Venus/CFP ratios in cells expressing NS5A-AT1.03^{YEMK} were markedly higher than those of NS5A-AT1.03 (Figure 5A; lower). In contrast, cells replicating SGR-AT1.03 and SGR-AT1.03^{YEMK} showed foci of brightly fluorescent dot-like structures in the cytoplasm (Figure 5B; upper panels). Interestingly, some of these fluorescent foci had an apparently higher Venus/

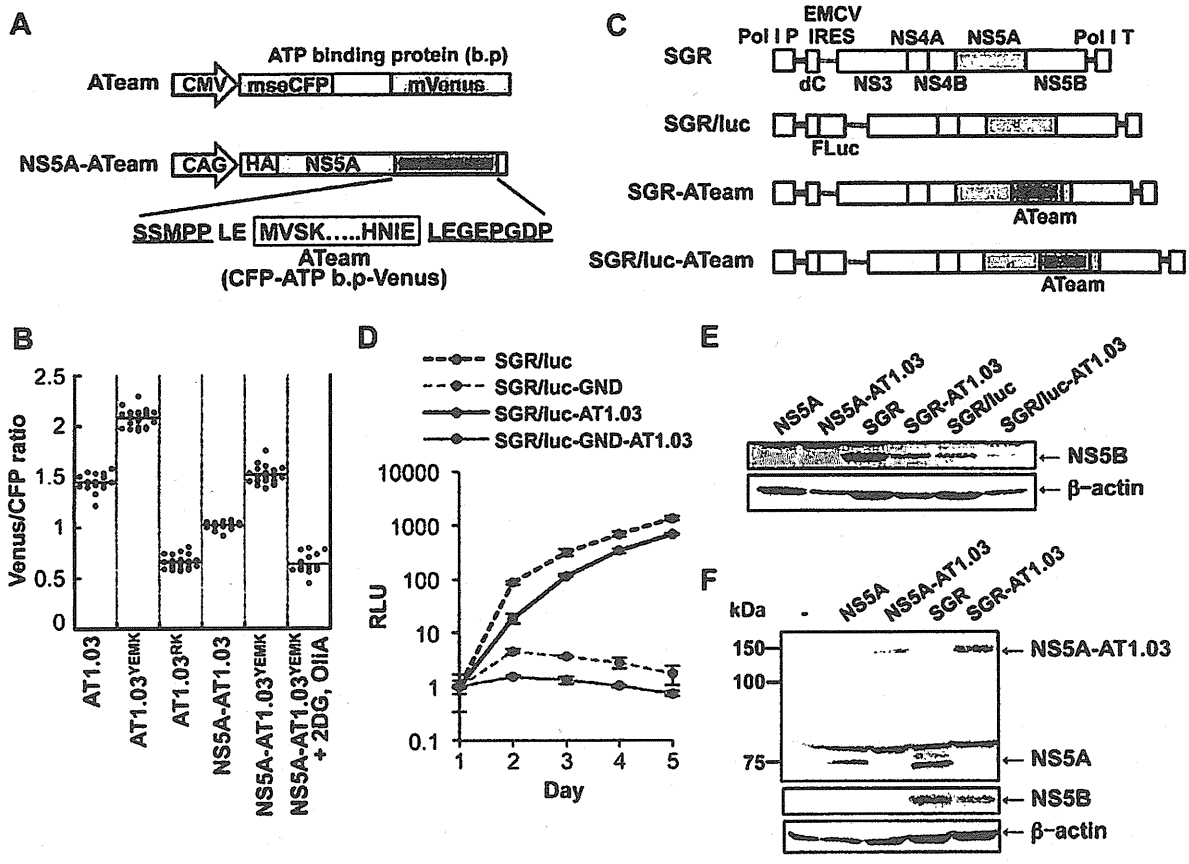

Figure 4. Development of NS5A-ATeam and SGR-ATeam to enable real-time monitoring of ATP. (A) Schematic representation of the ATeam and NS5A-ATeam used in this study. ATeam genes were inserted into the 3′ region of a HA-NS5A expression vector to generate NS5A-ATeam. The underlined sequences indicate NS5A residues. The insertion site was between residues 2394 and 2395, numbered according to the polyprotein of the HCV JFH-1 isolate. CMV, Cytomegalovirus promoter; CAG, CAG promoter; ATP b.p, ATP binding protein. HA, HA tag. (B) Huh-7 cells were transfected with ATeam and NS5A-ATeam constructs. Forty-eight hours post-transfection, the Venus/CFP ratios of each cell were calculated from fluorescent images acquired with a confocal microscope in the same way as described in the legends for Figure 2. Each plot shows the ratio of individual cells. Horizontal lines represent means. (C) Schematic representation of the SGR and SGR-ATeam plasmids used, with or without the firefly luciferase gene (Fluc). HCV polyproteins are indicated by the open boxes. ATeam genes were inserted into the same site in the NS5A C-terminal region. Bold lines indicate the HCV UTR. EMCV IRES is denoted by the gray bars. Pol I P, Pol I promotor; dC, 5′ region of Core gene; Pol I T, Pol I terminator. (D) Replication levels of SGR/luc-AT1.03 in transfected cells were determined by luciferase assay 1–5 days post-transfection. SGR/luc and SGR/luc-GND were used as positive and negative controls, respectively. Values given were normalized for transfection efficiency with luciferase activity determined 24 h post-transfection. All data are presented as means and SD for three independent samples. (E) Huh-7 cells were transfected with constructs encoding NS5A, NS5A-AT1.03, SGR, SGR-AT1.03, SGR/luc or SGR/luc-AT1.03, followed by immunoblotting with anti-NS5B or anti-beta-actin antibody. (F) Cells transfected with constructs encoding NS5A, NS5A-AT1.03, SGR or SGR-AT1.03 were analyzed by immunoblotting with anti-NS5A, anti-NS5B or anti-beta-actin antibodies.
doi:10.1371/journal.ppat.1002561.g004

CFP ratio than the surrounding cytoplasmic region (Figure 5B; middle and lower panels). Although the number of high Venus/CFP ratios was not consistent between the cells, this phenotype was observed in most of the cells that were replicating SGR-AT1.03 (Figure S3). Such high focal Venus/CFP ratios were not detected in cells replicating SGR-AT1.03^{RK} or in SGR-AT1.03^{YEMK} -replicating cells treated with 2DG and OliA. Thus, foci with a high Venus/CFP ratio apparently represent the presence of high ATP levels at distinct sites in cells replicating HCV RNA. In addition, when a replication-defective polyprotein that extended from NS3 through to the NS5B protein, including NS5A-AT1.03, was expressed, no high Venus/CFP ratio was seen in the cells in spite of the fact that NS5A-AT1.03 was detected in dot-like structures throughout the cytoplasm (Figure S4). These results strongly suggest that the high Venus/CFP ratios observed using the SGR-ATeam system are associated with the replication of HCV RNA.

To investigate whether the high Venus/CFP ratios of the dot-like structures detected in cells replicating SGR-ATeam are located at the HCV RC, FRET images of SGR-AT1.03-replicating cells were analyzed, followed immunofluorescence analysis of cells fixed and stained with either anti-NS5A or anti-NS3 antibodies (Figure 5C). Confocal fluorescence microscopy at high magnification demonstrated that the high Venus/CFP ratios that were identified in foci of various sizes were co-localized with NS5A and NS3 that were possibly membrane-bound within the cytoplasm of the viral replicating cells. Some of the NS3- or NS5A-labeled proteins that were identified by immunofluorescence were not associated with high Venus/CFP ratios. These results are consistent with previous reports, which demonstrated that only

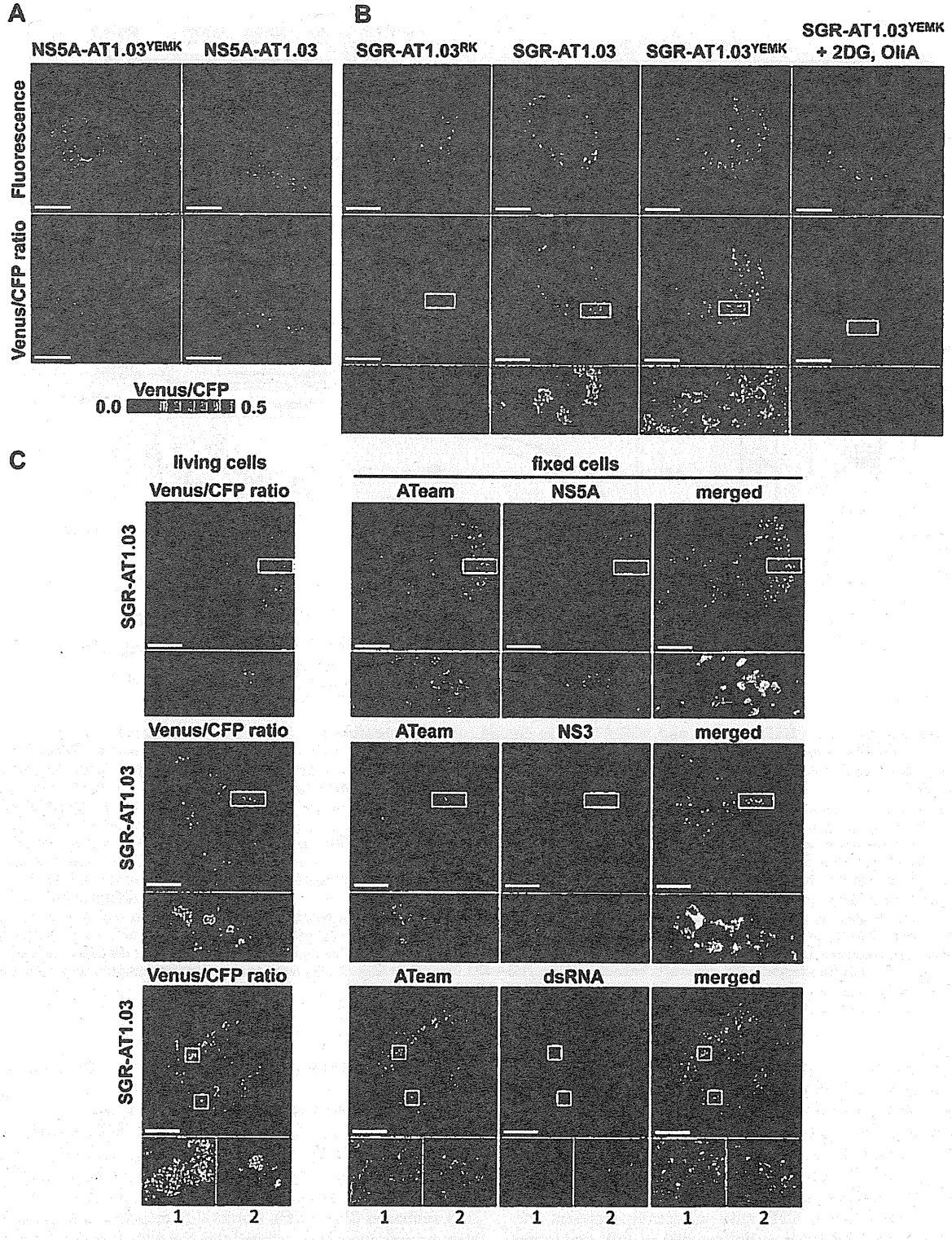

Figure 5. Visualization of sites of focal accumulation of ATP in cells expressing NS5A-ATeam or SGR-ATeam. (A) Huh-7 cells were transfected with NS5A-AT1.03 or NS5A-AT1.03^{YEMK}. Four days after transfection, the cells were analyzed using spectral imaging (405-nm excitation) of LSM510-META (Carl Zeiss). Images were processed to the CFP channel (F_{CFP}) and the Venus channel (F_{Venus}) using a linear unmixing algorithm using a reference for each spectrum. The upper panels demonstrate the signal intensity from a spectral channel with maximum intensity and represent the expression pattern of NS5A-ATeam. The lower panels are constructed from FRET ratio images (F_{CFP}/F_{Venus}) with pseudocolors. The pseudocolor scale is shown below. Scale bars, 20 μm. (B) Huh-7 cells were transfected with SGR-AT1.03^{RK}, SGR-AT1.03 or SGR-AT1.03^{YEMK}, and were analyzed in the same

way as described in (A). SGR-AT1.03^{YEMK} -transfected cells were treated with 10 mM 2DG and 10 μg/ml OliA just before imaging and were used as a negative control. The upper panels demonstrate the intensity from a spectral channel with maximum intensity and represent the expression pattern of NS5A-ATeam processed from SGR-ATeam. The lower panels indicate square areas within FRET ratio panels magnified five-fold. Scale bars, 20 μm. (C) Cells were fixed after live-cell FRET imaging, and the same cell was analyzed by indirect immunofluorescence staining. Viral proteins were labeled with antibodies against NS5A (upper panels), NS3 (middle panels) and dsRNA (lower panels), which were detected with an Alexa Fluor 555-labeled anti-rabbit or anti-mouse antibody. ATeam panels (green) represent the expression of NS5A-ATeam processed from SGR-ATeam, and NS5A, NS3 or dsRNA panels (red) represent the immunostained signals. Enlarged views of the areas outlined by squares at a five-fold magnification are also shown. Scale bars, 20 μm.
doi:10.1371/journal.ppat.1002561.g005

some of the expressed HCV NS proteins contribute to viral RNA synthesis [27]. To further investigate the relationship between the cellular sites at which there was a high Venus/CFP ratio and HCV RNA replication, double-stranded RNA (dsRNA) was visualized by staining with a specific anti-dsRNA antibody after FRET imaging (Figure 5C). This staining indicated that dsRNA-containing dot-like structures co-localized with structures that displayed high Venus/CFP ratios. Therefore, it is most likely that the dot-like structures with high Venus/CFP ratios that were detected using the SGR-ATeam system reflect the sites of HCV RNA replication or HCV RCs.

Several studies have shown that mitochondria, which play a central role in ATP metabolism, localize to areas near the membranous web, the likely site of HCV RNA replication [28]. We thus compared the subcellular localization of the fluorescence signals detected in cells expressing SGR-ATeam with that of mitochondria that were visualized by staining with Mitotracker. Foci with high Venus/CFP ratios did not colocalize with, but were localized adjacent to mitochondria in cells that were replicating SGR-AT1.03 (Figure S5). This finding might reflect the fact that ATP can be directly supplied from mitochondria to the sites of viral RNA replication in cells.

Quantification of ATP at putative cytoplasmic sites of HCV RNA replication within cells

Based on the above observations, FRET signals detected within cells expressing SGR-ATeam or NS5A-ATeam can be classified as either signals from distinct dot-like structures, which represent putative subcellular sites of HCV RNA replication, or as signals that are diffuse throughout the cytoplasm. The Venus/CFP emission ratio in individual cells into which NS5A-AT1.03, NS5A-AT1.03^{YEMK}, SGR-AT1.03, SGR-AT1.03^{YEMK} or SGR-AT1.03^{RK} was introduced was determined (Figure 6A). Fluorescent signals corresponding to cytoplasmic ATP were identified by subtracting signals at putative sites of viral RNA replication from signals from the cytoplasmic area as a whole. Cytoplasmic Venus/CFP ratios within cells replicating SGR-AT1.03 and SGR-AT1.03^{YEMK} were lower than those in cells expressing NS5A-AT1.03 and NS5A-AT1.03^{YEMK}, respectively. Therefore, cytoplasmic ATP levels within HCV RNA-replicating cells were lower than in non-replicating cells. This result is consistent with the findings shown in Figure 1A. The average Venus/CFP ratios at potential sites of viral RNA replication were greater than the corresponding cytoplasmic levels in cells replicating SGR-AT1.03 or SGR-AT1.03^{YEMK}. As expected, a significant decrease in Venus/CFP ratios was observed in cells treated with 2DG and OliA.

We next quantified ATP levels within individual cells replicating HCV RNA based on the Venus/CFP ratios obtained. To generate standard curves for this calculation, permeabilized cells expressing NS5A-AT1.03 or NS5A-AT1.03^{YEMK} were prepared by digitonin treatment, followed by the addition of defined concentrations of ATP and subsequent FRET analysis [29,30]. As shown in Figure 6B, under these experimental conditions, baseline Venus/CFP ratios of approximately 0.1 were detected in the absence of exogenous ATP, and Venus/CFP ratios were observed to increase linearly with increasing ATP concentration. The standard curves thus obtained can be used to estimate the ATP concentrations of unknown samples in which a particular ATeam containing an ATP probe at the C terminus of HCV NS5A, such as NS5A-ATeam or SGR-ATeam, have been introduced. Based on the fluorescent signal obtained in cells replicating SGR-ATeam, as well as in cells expressing NS5A-ATeam, the ATP concentration at putative sites of HCV RNA replication was estimated to be ~5 mM in the experiments shown in Figures 5A and 5B (average value of putative replication sites; 4.8 mM). After subtraction of the ATP that was localized at the HCV replication sites, the ATP concentration of HCV-replicating SGR cells (~1 mM) was found to be approximately half that observed in parental non-replicating cells (~2 mM)(average values in SGR and parental cells; 0.8 mM and 2.2 mM, respectively). To our knowledge, this is the first experiment in which ATP levels were estimated inside living cells during viral genome replication.

Figures 5 and 6A demonstrate changes in ATP concentrations at distinct sites in cells undergoing HCV RNA replication. Finally, we determined the effect of the PSI-6130 inhibitor of HCV replication on the change in subcellular ATP concentration in cells following introduction of SGR-AT1.03, SGR-AT1.03^{RK} or NS5A-AT1.03 (Figure 6C). In general, nucleoside analogue inhibitors of viral replication prevent RNA/DNA synthesis by chain termination immediately after addition to infected cells [23]. Indeed, as shown in Figure 3, a decrease in ATP consumption was detected even following a PSI-6130 treatment period as short as 15 min of permeabilized HCV replicon cells. We therefore analyzed and estimated ATP levels in cells in the presence of PSI-6130 for 10 min and 2 h. ATP concentrations at putative sites of viral RNA replication, as well as cytoplasmic ATP levels, were higher in SGR-AT1.03-replicating cells in the presence of 0.1–5 μM PSI-6130 for 10 min compared to the same cells without inhibitor treatment or to NS5A-AT1.03-expressing cells. A dose-dependent PSI-6130-induced increase in ATP levels at the putative replication sites was observed under the condition used. By treatment with PSI-6130 for 2 h, the ATP levels at putative replication sites were significantly lower than those without inhibitor treatment in SGR-AT1.03-replicating cells. The cytoplasmic ATP levels were similar with or without 2-h treatment (Figure 6C). In HCV SGR-ATeam cells treated with PSI-6130 for 3 days, HCV RNA replication was dramatically inhibited by greater than 90% with no observed cytotoxicity (Figure S6) and, as expected, little or no high Venus/CFP signal was detected anywhere in the cells (data not shown). We adapted the ATeam system to monitor ATP in HCV RNA replicating cells and found increased ATP levels at the putative subcellular sites of the viral replication. Findings obtained from experiments using the viral polymerase inhibitor strongly suggest that changes in ATP concentrations at the distinct sites observed depend on the viral RNA replication.

Discussion

This paper is the first to demonstrate changes in ATP within cells during viral genome replication. ATP requirements during

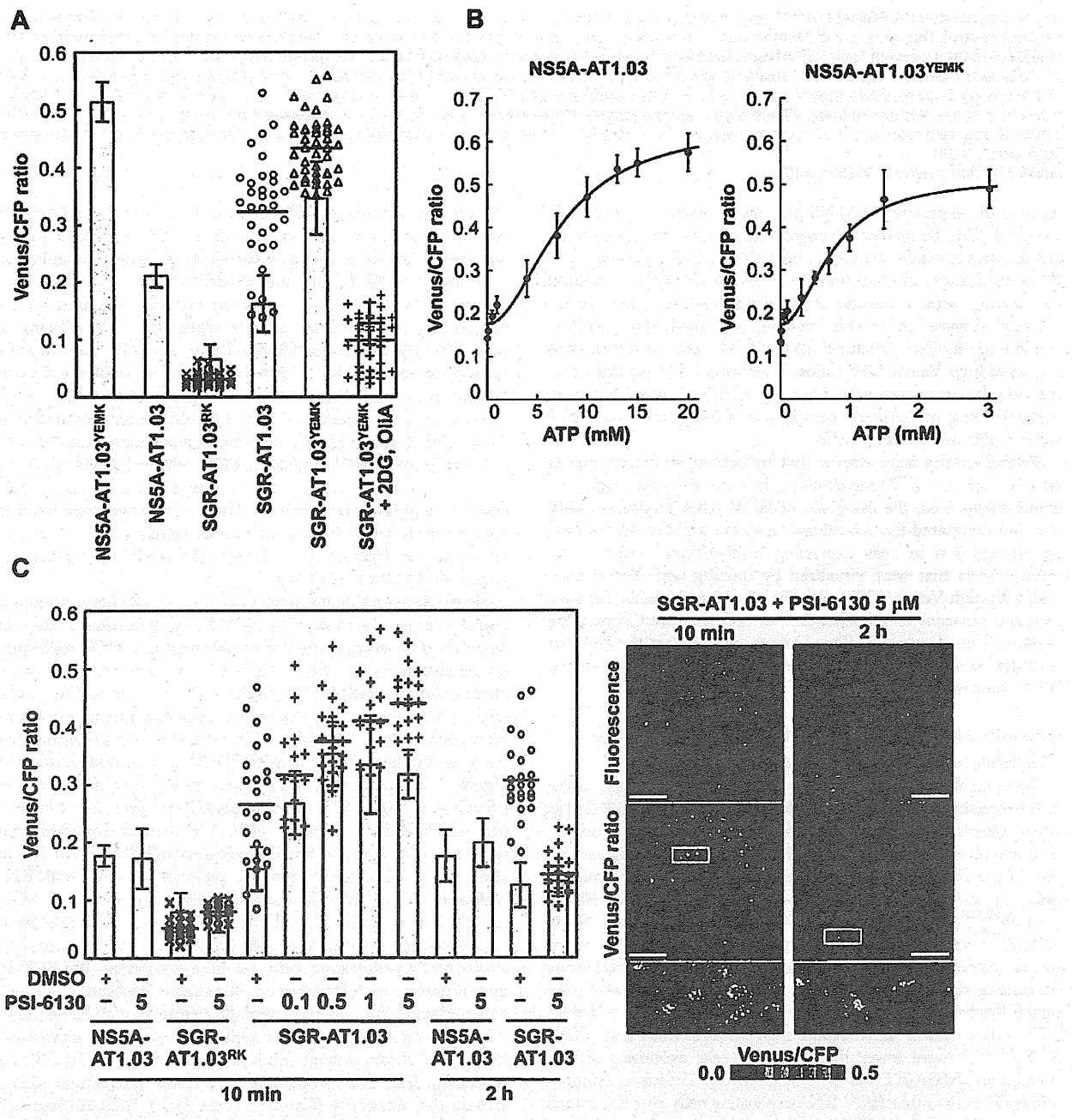

Figure 6. Estimation of ATP levels at possible sites of HCV RNA replication in living cells. (A) Venus/CFP emission ratios were calculated from images of CFP and Venus channels in individual cells for each group. Bar- and dotted graphs indicate ratios within the cytoplasm and ratios for dot-like structures, respectively, in the same cells, as shown in Figures 5A and 5B. Data in bar graphs are indicated as means and SD. Horizontal lines in the dot graphs denote means from at least three independent cells. Values in the cytoplasm of cells transfected with NS5A-AT1.03^{YEMK} and SGR-AT1.03^{YEMK} were statistically significant ($p<0.05$) as evaluated using the Student's *t*-test. (B) Calibration of NS5A-ATeam in cells under semi-intact conditions. Cells were transfected with NS5A-AT1.03 and NS5A-AT1.03^{YEMK}, respectively. Forty-eight hours later, the cells were permeabilized, followed by addition of known concentrations of ATP. FRET analyses were performed as described in Figure 5A. Each trace represents mean with SD of at least six independent cells. Plots were fitted with Hill equations with a fixed Hill coefficient of 2; $R=(R_{max}-R_{min})\times[ATP]^2/([ATP]^2+Kd^2)+R_{min}$, where R_{max} and R_{min} are the maximum and minimum fluorescence ratios, respectively. *Kd* is the apparent dissociation constant. R values were 0.994 and 0.986 for NS5A-AT1.03 and NS5A-AT1.03^{YEMK}, respectively. (C) Cells were transfected with NS5A-AT1.03, SGR-AT1.03^{RK} or SGR-AT1.03. The cells were then treated with PSI-6130 at indicated concentrations (μM) for 10 min or 2 h, and were analyzed as described in (A). Values in the cytoplasm of cells transfected with SGR-AT1.03 with and without PSI-6130 treatment were statistically significant ($p<0.05$ for control versus 0.1 or 1 μM PSI-6130, $p<0.01$ for control versus 0.5 or 5 μM PSI-6130) as evaluated using the Student's *t*-test. Representative cells treated with 5 μM PSI-6130 are shown in the right panel. The lower panel is a five-fold magnification of the boxed area. Scale bars, 20 μm.
doi:10.1371/journal.ppat.1002561.g006

the virus lifecycle have been studied for years. Several key steps during the viral life cycle, such as genome synthesis, require high-energy phosphoryl groups. For instance, it has been shown that ATP is required for the formation of a preinitiation complex for de novo RNA synthesis by RdRp of flaviviruses [31]. Transcriptional initiation and RNA replication by influenza virus RdRp are functional in an ATP-dependent fashion [32,33]. An ATP requirement of viral helicase activities has also been reported [34]. Furthermore, it has been demonstrated that ATP is involved in the assembly and/or release of viral structural proteins possibly via interaction with ATP-dependent chaperones [35,36]. However, it has been controversial as to whether ATP can be concentrated in particular subcellular compartment(s) in infected cells during viral replication. One of the underlying reasons for this controversy may be that a method by which cellular ATP levels can be determined, apart from examination of ATP levels in cellular extracts in the steady-state, has been lacking [37]. Recently Imamura et al. established FRET-based indicators, known as ATeams, for ATP quantification, and have shown that the use of ATeams enables the monitoring of ATP levels in real-time in different cellular compartments within individual cells [2].

In this study, in order to visualize and monitor ATP levels in living cells during replication of the viral genome, we first introduced the original ATeam-expressing plasmids into cells and found that cytoplasmic ATP levels in cells undergoing HCV genotype 1b and 2a RNA replication were lower than those in cured or parental cell lines (Figures 2 and S2). These results agree with the results of CE-TOF MS analysis (Figure 1) and the ATP consumption assay (Figure 3). It is therefore likely that ATP is actively consumed in cells during viral RNA replication, resulting in reduced levels of ATP in the cytoplasm. Furthermore, NS5A-ATeam fusion constructs, in which the ATeam gene was introduced into the C-terminal end of the NS5A coding region, and SGR-ATeam constructs containing a HCV JFH-1-derived subgenomic replicon within the NS5A-ATeam fused sequence as described above, were engineered (Figure 4). The results obtained using several ATeam fusion constructs with different affinities for ATP indicated that NS5A-ATeam fusion constructs can be used as FRET-based ATP indicators, and that the ATeam-tagged HCV replicons are capable of transient replication of viral RNA (Figure 4). It is interesting that our experiment using a SGR-ATeam construct provides evidence for the formation of ATP-enriched foci within cells that support HCV RNA replication (Figures 5 and 6). FRET-signal detection followed by indirect immunofluorescence allowed us to visualize co-localization of viral proteins as well as dsRNA at sites of ATP accumulation in cells (Figure 5), suggesting that these membrane-associated ATP-enriched foci likely represent sites of HCV RNA replication in transient replication assays.

Attempting to precisely quantify ATP within individual cells or particular intracellular compartments is a very challenging process. The luciferin-luciferase reaction has been utilized to monitor cellular ATP levels by measuring the released photon count during catalysis of bioluminescent oxidation by firefly luciferase. A previous study based on the luciferin-luciferase assay estimated basal cytoplasmic ATP levels at ~1.3 mM, which increased to ~5 mM during apoptotic cell death [38]. However, the results obtained were likely influenced by cellular levels of luciferase and other assay components, as well as by the pH of the cells. In this study, we describe quantification of ATP in human hepatoma Huh-7 cells undergoing HCV RNA replication using SGR-ATeam technology. Although ATP requirements during the lifecycles of various viruses have been studied for years, the use of ATeam technology enabled us, for the first time, to evaluate ATP concentrations at sites of viral replication within living cells. We here demonstrate that ATP concentrations at these putative subcellular sites of HCV RNA replication approach ~5 mM (Figure 6). This ATP level is as high as that observed during apoptotic processes such as caspase activation and DNA fragmentation, even though the latter ATP level was determined using a different assay system [38]. Considering that these apoptotic events were not observed at basal ATP levels [38], replication of the viral genome likely also requires high concentrations of cellular ATP. It should be noted that, in contrast to the fluorescent reporter system traditionally used to calculate the ATP/ADP ratio [39], the bacterial epsilon subunit used in ATeam is highly specific for ATP, but not for other nucleotides such as ADP, CTP, GTP or UTP [2,3]. In evaluating the effect of the HCV polymerase inhibitor on changes in the subcellular ATP concentration in cells replicating SGR-ATeam, an increase in ATP concentration was observed both at putative replication sites and in the cytoplasm of SGR-AT1.03-replicating cells in the presence of PSI-6130 for 10 min (Figure 6C). By contrast, 2-h treatment with the inhibitor resulted in reduction of ATP levels at putative replication sites in the replicon cells. Although the result of the experiment with 10-min treatment may be somewhat unexpected, it might possibly be explained by the following hypothesis. PSI-6130 began to inhibit viral RNA synthesis, leading to a decrease in ATP consumption. Since a mechanism for ATP transport mediated by host cell and/or viral factor(s) is still active during this time period, the ATP level at the replication sites should be increased compared to that during active replication. Higher levels of metabolic intermediates for glyconeogenesis as well as for glycolysis in HCV-infected cells compared to non-infected cells as determined via metabolome analysis (data not shown) may also be implicated in the increased ATP levels at the initial stage of inhibition of HCV replication. It is likely that active consumption of ATP caused by HCV replication and ATP transportation into the replication sites would lead to reduction of cytoplasmic ATP level. Such a change in ATP balance may result in induction of ATP generation and increase in certain metabolic intermediates related to glucose metabolism. These metabolome responses are supposed to maintain in short-term (10 min) treatment with PSI-6130. Thus, inhibition of HCV RNA replication by PSI-6130 under the conditions used may lead to increase in the cytoplasmic ATP level. It is likely that these metabolome responses were not observed after the longer-term (2 h) treatment presumably because the viral replication was inhibited by the inhibitor for a sufficient period of time. Further study is required to address the molecular mechanism underlying change in ATP balance caused by HCV replication and the viral inhibitors.

The mechanism by which ATP accumulates at potential sites of HCV RNA replication remains unclear. We have previously demonstrated that creatine kinase B (CKB), which is an ATP-generating enzyme and maintains cellular energy stores, accumulates in the HCV RC-rich fraction of viral replicating cells [22]. Our earlier results suggest that CKB can be directed to the HCV RC via its interaction with the HCV NS4A protein and thereby functions as a positive regulator for the viral replicase by providing ATP [22]. One may hypothesize that recruitment of the ATP generating machinery into the membrane-associated site, through its interaction with viral proteins comprising the RC, is at least in part linked with elevated concentrations of ATP at a particular site. Through our preliminary study, however, subcellular ATP distribution was not changed significantly in replicon cells where HCV RNA replication was reduced ~50% by siRNA-mediated knockdown of the CKB gene (data not shown). Another possibility

may be implication of communication between mitochondria and membrane-enclosed structures of HCV RC in ATP transport through membrane-to-membrane contact. As indicated in Figure S5, putative sites of the viral RNA replication with high Venus/CFP ratios were mainly localized proximal to mitochondria. Studies are ongoing to understand the mechanism(s) underlying this phenomenon, as well as to determine if changes in ATP levels at intracellular sites supporting replication might also be observed for other RNA or DNA viruses.

In summary, we have used a FRET-based ATP indicator called ATeam to monitor ATP levels in living cells where viral RNA replicates by designing HCV replicons harboring wild-type or mutated ATeam probes inserted into the C-terminal domain of NS5A. We evaluated changes in ATP levels during HCV RNA replication and demonstrated elevated ATP levels at putative sites of replication following detection of FRET signals, which appeared as dot-like foci within the cytoplasm. The ATeam system may become a powerful tool in microbiology research by enabling determination of subcellular ATP localization in living cells infected or associated with microbes, as well as investigation of the regulation of ATP-dependent processes during the lifecycle of various pathogens.

Materials and Methods

Chemicals

PSI-6130 (β-D-2′-Deoxy-2′-fluoro-2′-*C*-methylcytidine) and recombinant human IFN-alpha2b were obtained from Pharmasset Inc. (Princeton, NJ) [23,24] and Schering-Plough (Kenilworth, NJ), respectively. OliA and 2DG were purchased from Sigma-Aldrich (St. Louis, MO). ATP used in this study was complexed with equimolar concentrations of magnesium chloride before use in the experiments.

Plasmids

The construction of the ATeam plasmids pRSET-AT1.03, pRSET-AT1.03^{YEMK} and pRSET-AT1.03$^{R122K/R126K}$, which express wild-type ATeam (AT1.03), as well as a high-affinity mutant (AT1.03^{YEMK}) and a non-binding mutant (AT1.03^{RK}), has been previously described [2]. pHH/SGR-Luc (also termed SGR/luc) contains cDNA of a subgenomic replicon of HCV JFH-1 isolate (genotype 2a; [14]) with firefly luciferase flanked by the Pol I promoter and the Pol I terminator, yielding efficient RNA replication upon DNA transfection [26]. pHH/SGR-Luc/GND (also termed SGR/luc-GND), in which a point mutation of the GDD motif of the NS5B was introduced in order to abolish RNA-dependent RNA polymerase activity, was used as a negative control. pHH/SGR (also termed SGR) was created by deleting the luciferase gene in pHH/SGR-Luc. To generate a series of SGR-ATeam plasmids, wild-type or mutant ATeam genes were inserted into pHH/SGR-Luc or pHH/SGR at the Xho I site of NS5A (between amino acids 418 and 419) [25]. The ATeam genes were also inserted into the same site of pCAGNS5A, which contains the NS5A gene of JFH-1 downstream of the CAG promoter and hemagglutinin (HA) tag [26], yielding NS5A-ATeam plasmids. To generate a plasmid expressing NS3-NS5B-AT1.03 under the control of the CAG promoter, a DNA fragment containing the coding region of NS3/NS4A/NS4B/NS5A-AT1.03/NS5B of SGR/luc-ATeam was inserted into the pCAGGS vector [40]. Exact cloning strategies are available upon request.

Cell culture and plasmid transfection

Human hepatoma Huh-7 cells were propagated in Dulbecco's modified Eagle's medium (DMEM) supplemented with 10% fetal calf serum (FCS) as well as minimal essential medium non-essential amino acid (MEM NEAA)(Invitrogen, Carlsbad, CA) in the presence of 100 units/ml of penicillin and 100 μg/ml of streptomycin. The Huh-7-derived cell lines JFH-1/4-1 and JFH-1/4-5, which support replication of SGR RNA of HCV JFH-1 (genotype 2a) and NK5.1/0-9, which carries the SGR RNA of Con1 NK5.1 (genotype 1b), were cultured and maintained under previously described conditions [15]. DNA transfection was performed using a TransIT-LT1 transfection reagent (Takara, Shiga, Japan) in accordance with the manufacturer's instructions.

CE-TOF MS analysis

Huh-7 cells were mock-infected or infected with HCVcc derived from a wild-type JFH-1 isolate at a multiplicity of infection of 1. When most cells had become virus positive, as confirmed by immunofluorescence, with no observable cell damage at 9 days post-infection, equal amounts of cells with and without HCV infection were scraped with MeOH including 10 μM of an internal standard after washing twice with 5% mannitol solution. Replicon cells (JFH-1/4-5) that were cultured in the absence of G418 for 2 days were harvested and prepared as above. The extracts were mixed with chloroform and water, followed by centrifugation at 2,300× *g* for 5 min at 4°C, The upper aqueous layer was centrifugally filtered through a 5-kDa cutoff filter to remove proteins. The filtrate was lyophilized and dissolved in water, then subjected to CE-TOF MS analysis. CE-TOF MS experiments were performed using an Agilent CE-TOF MS system (Agilent Technologies, Waldbronn, Germany) as described previously [41].

ATP consumption assay

The ATP consumption assay using permeabilized replicon cells was carried out as previously described [13,22] with slight modifications, so that it was unnecessary to add either exogenous phosphocreatine or creatine phosphokinase to minimize ATP reproduction in cells. Cells (2×10^6) cultured in the presence or absence of PSI-6130 for 72 h were treated with 5 μg Actinomycin D/ml, followed by trypsinization and 3 washes with cold buffer B (20 mM HEPES-KOH [pH 7.7], 110 mM potassium acetate, 2 mM magnesium acetate, 1 mM EGTA, and 2 mM dithiothreitol). The cells were permeabilized by incubation with buffer B containing 50 μg/ml digitonin for 5 min on ice and the reaction was stopped by washing 3 times with cold buffer B. The permeabilized cells (1×10^5) were resuspended with 100 μl buffer B containing 5 μM ATP, GTP, CTP, and UTP, 20 μM $MgCl_2$, and 5 μg/ml Actinomycin D. After incubation at 27°C for 15 min, samples were centrifuged, and 20 μl of the supernatant was then mixed with 5 μl of 5× passive lysis buffer (Promega, Madison, WI). The ATP level was determined using a CellTiter-Glo Luminescent cell viability assay system (Promega). All assays were performed at least in triplicate.

Live cell microscopy

Plasmids carrying the ATP indicators were transfected at 48 h (ATeam and NS5A-ATeam) or 4 days (SGR-ATeam) before imaging of the cells. One day before imaging, the cells were seeded onto 30-mm glass-bottomed dishes (AGC Techno Glass, Chiba, Japan) at about 60% confluency. For imaging, the cells were maintained in phenol red-free DMEM containing 20 mM HEPES-KOH [pH 7.7], 10% FCS and MEM NEAA.

Two kinds of confocal microscopies were used to perform the FRET analysis in this study as follows. Since the ways of acquisition of each spectrum were quite different between the two microscopies, differences in the values of the Venus/CFP ratios in different

experiments were observed. In Figures 2, 4B and S2, cells were imaged using a confocal inverted microscope FV1000 (Olympus, Tokyo, Japan) equipped with an oil-immersion 60× Olympus UPlanSApo objective (NA = 1.35). Cells were maintained on the microscope at 37°C with a stage-top incubation system (Tokai Hit, Shizuoka, Japan). Cells were excited by a 405-nm laser diode, and CFP and Venus were detected at 480–500 nm and 515–615 nm wavelength ranges, respectively. In the analysis shown in Figures 5, 6, S3, S4 and S5, FRET images were obtained using a Zeiss LSM510 Meta confocal microscope with an oil-immersion 63× Zeiss Plan-APOCHROMAT objective (NA = 1.4)(Carl Zeiss, Jena, Germany). Cells were maintained on the microscope at 37°C with a continuous supply of a 95% air and 5% CO_2 mixture using a XL-3 incubator (Carl Zeiss). Cells were excited by a 405-nm blue diode laser, and emission spectra of 433–604 nm wavelength range were obtained using an equipped scanning module (META detector) [42,43]. Images were computationally processed by a linear unmixing algorithm using the reference spectrum of CFP and Venus, which were obtained from individual fluorescence-expressing cells. All image analyses were performed using MetaMorph (Molecular Devices, Sunnyvale, CA). Fluorescence intensities of cytoplasmic areas in NS5A-ATeam transfected cells were calculated by subtraction of the signal intensities of the nucleus from the signal intensities of the whole cell, which was standardized by the area of the corresponding cytoplasmic region. Fluorescence intensities of cytoplasmic areas and at dot-like structures corresponding to the putative viral replicating sites in SGR-ATeam-transfected cells were measured and calculated as follows. All pixels above CFP intensity levels of 100–200 were selected. The positions of dot-like structures were then determined by examining areas greater than 0.5×10^{-12} square meters and the intensity of each dot was measured. The fluorescence intensity of the cytoplasmic area, excluding that of the putative viral replicating sites in each cell, was calculated by subtraction of the signal intensities of the nucleus and the dot-like structures, as determined above, from the signal intensity of the whole cell, which was standardized by the area of the corresponding cytoplasmic region. Each Venus/CFP emission ratio was calculated by dividing pixel-by-pixel a Venus image with a CFP image.

To investigate the relationship between Venus/CFP ratios and ATP concentrations in cells, calibration procedures were performed according to previous reports [29,30]. Huh-7 cells were transfected with NS5A-AT1.03 or NS5A-AT1.03^{YEMK}. Forty-eight hours later, the cells were permeabilized by incubation with buffer B containing 50 μg/ml digitonin for 5 min at room temperature. The reaction was stopped by washing 3 times with buffer B, followed by the addition of known concentrations of ATP in warmed medium for imaging. FRET analysis, with calibration of the signal intensity in the cytoplasm of each cell, was performed as described above. Plots were fitted with Hill equations with a fixed Hill coefficient of 2; $R=(R_{max}-R_{min})\times[ATP]^2/([ATP]^2+Kd^2)+R_{min}$, where R_{max} and R_{min} are the maximum and minimum fluorescence ratios, respectively and Kd is the apparent dissociation constant.

To analyze the effect of an inhibitor against HCV NS5B polymerase, the medium for the cells replicating SGR-ATeam was changed to medium containing various concentrations of PSI-6130. After 10-min incubation at 37°C under a continuous supply of 95% air and 5% CO_2, fluorescence intensities of cytoplasmic areas and at dot-like structures were determined as described above. Medium containing 0.01% DMSO was used as a negative control.

To visualize mitochondria, MitoTracker Red CMXRos (Molecular Probes, Eugene, OR) was added to the culture medium to a final concentration of 100 nM, incubated for 15 min at 37°C and the cells were then washed twice with phosphate buffered saline (PBS) before FRET analysis of living cells. Images were computationally processed as described above. The reference spectrum of MitoTracker Red CMXRos was obtained from stained parental, non-transfected, Huh-7 cells.

Indirect immunofluorescence

Cells expressing SGR-ATeam were cultured in 30-mm glass-bottomed dishes with an address grid on the coverslip (AGC Techno Glass). After FRET analysis of living cells as described above, the cells were fixed with 4% paraformaldehyde at room temperature for 30 min. After washing with PBS, the cells were permeabilized with PBS containing 0.3% Triton X-100 and individually stained with a rabbit polyclonal antibody against NS3 [44], an anti-NS5A antibody [45], or a mouse monoclonal antibody against dsRNA antibody (Biocenter Ltd., Szirak, Hungary) [46]. The fluorescent secondary antibody used was Alexa Fluor 555-conjugated anti-rabbit- or anti-mouse IgG (Invitrogen). The cells were imaged using a Zeiss LSM510 Meta confocal microscope with an oil-immersion 63× Zeiss Plan-APOCHROMAT objective (NA = 1.4). For dual-color imaging, the ATeam signal was excited with the 488-nm laser line of an argon laser and Alexa Fluor 555 was excited with a 543-nm HeNe laser under MultiTrack mode. Emission filters with a 505- to 530-nm band-pass and 560-nm-long pass filter were used.

Luciferase assay

Huh-7 cells transfected with SGR/luc or SGR/luc-ATeam were harvested at different time points after transfection (Figure 4D) or at 3 days after treatment with PSI-6130 (Figure S6) and lysed in passive lysis buffer (Promega). To monitor HCV RNA replication, the luciferase activity in cells was determined using a Luciferase Assay system (Promega). All assays were performed at least in triplicate.

MTT assay

Cell viability was assessed using the Cell Proliferation Kit II (Roche, Indianapolis, IN) according to the manufacturer's instructions. The kit measures mitochondrial dehydrogenase activity, which is used as a marker of viable cells, using a colorimetric sodium3′-[1(-phenylaminocarbonyl)-3,4-tetrazolium]-bis(4-methoxy-6-nitro)benzene sulfonic acid hydrate (MTT) assay.

Quantification of HCV RNA

HCV RNA copies in the replicon cells with or without PSI-6130 treatment were determined using the real-time detection reverse transcription polymerase chain reaction (RTD-PCR) described previously [47] with the ABI Prisom 7700 sequence detector system (Applied Biosystems Japan, Tokyo, Japan).

Western blotting

The proteins were transferred onto a polyvinylidene difluoride membrane (Immobilon; Millipore, Bedford, MA) after separation by SDS-PAGE. After blocking, the membranes were probed with a rabbit polyclonal anti-NS5A antibody [44], a rabbit polyclonal anti-NS5B antibody (Chemicon, Temecula, CA), or a mouse polyclonal anti-beta-actin antibody (Sigma-Aldrich), followed by incubation with a peroxidase-conjugated secondary antibody and visualization with an ECL Plus Western blotting detection system (GE Healthcare, Buckinghamshire, UK).

Supporting Information

Figure S1 ATP Levels in HCV replicon cells and parental Huh-7 cells determined by CE-TOF MS. ATP metabolites in Huh-7 cells and JFH-1/4-5 cells were measured by

CE-TOFMS. The values of each measurement are shown at left. The right graph shows means with SD of the data at left. Open bar; Huh-7 cells, gray bar; JFH-1/4-5 cells.
(TIF)

Figure S2 Cytoplasmic ATP levels in HCV replicon cells and IFN-treated cells. (Left) The HCV replicon cells JFH-1/4-1, JFH-1/4-5 (genotype 2a) and NK5.1/0-9 (genotype 1b), and parental Huh-7 cells were cultured for 72 h in the absence or presence of 1,000 IU/ml IFN-alpha. Forty-eight hours after transfection with AT1.03, the Venus/CFP emission ratio of each cell was calculated from fluorescent images acquired with the confocal microscope FV1000. All data are presented as means and SD for at least 10 independent cells. (Right) HCV RNA titers in cells corresponding to the left panel were determined using real-time quantitative RT-PCR. Data are presented as means and SD for three independent samples. NTD indicates not detected.
(TIF)

Figure S3 Increase in ATP-enriched dot-like structures in cells replicating SGR-ATeam. Huh-7 cells were transfected with SGR-AT1.03, and analyzed in the same way as described in the legends for Figures 5A and 5B. The lower four panels are five-fold magnifications of the boxed areas in independent cells. Scale bars, 40 μm.
(TIF)

Figure S4 Visualization of the ATP level in cells expressing replication-defective HCV polyprotein. (A) A schematic representation of the NS3-NS5B-AT1.03 plasmid is shown. The HCV polyprotein is indicated by the open boxes. The ATeam gene was inserted into the same site as that for NS5A-ATeam and SGR-ATeam insertion as indicated in the legend for Figure 4A. CAG, CAG promoter. (B) Cells transfected with constructs encoding NS5A, NS5A-AT1.03, NS3-NS5B-AT1.03, SGR or SGR-AT1.03 were analyzed by immunoblotting with anti-NS5A, anti-NS5B or anti-beta-actin antibodies. (C) Huh-7 cells were transfected with NS3-NS5B-AT1.03, and analyzed in the same way as described in the legends for Figures 5A and 5B. The upper panel (Fluorescence) demonstrates signal intensity from a spectral channel with maximum intensity and represents the expression pattern of NS5A-ATeam processed from NS3-NS5B-AT1.03. The lower panels (Venus/CFP ratio) indicate the FRET ratio and a five-fold magnification of the boxed area. Scale bar, 20 μm.
(TIF)

Figure S5 Relationship between ATP-enriched dot-like structures and mitochondria. Huh-7 cells replicating SGR-AT1.03 (right panels) and parental cells (left panel) were analyzed. Active mitochondria were labeled with MitoTracker Red CMXRos in living cells, and were analyzed in the same way as described in the legends for Figures 5A and 5B, using a reference for the MitoTracker spectrum. The lowest panels of SGR-ATeam cells indicate five-fold magnifications of the boxed areas. Scale bars, 20 μm.
(TIF)

Figure S6 Inhibitory effect of PSI-6130 on HCV RNA replication. (A) Replication levels of SGR/luc-AT1.03 RNA in transfected cells were determined by luciferase assay 3 days after treatment with PSI-6130 at the indicated concentrations (μM). The values shown were normalized for transfection efficiency with luciferase activity determined 24 h post-transfection. All data are presented as means and SD for three independent samples. (B) Cell viability was assessed using the MTT assay.
(TIF)

Acknowledgments

We are grateful to Minoru Tobiume, Tadaki Suzuki, Teruyuki Nagamune, Satoshi Yamaguchi, Yoshiharu Matsuura, Hiroto Kambara, Tomoko Date, Su Su Hmwe, Koichi Watashi, Takahiro Masaki and Takanobu Kato for their excellent technical assistance and advice, as well as to Takeharu Nagai for providing the mVenus expression vector and to Atsushi Miyawaki for providing the mseCFP expression vector. We thank our coworkers for their helpful discussions. We also thank Mami Sasaki for her technical assistance and Tomoko Mizoguchi for her secretarial work. We also thank the University of Tokyo Center for NanoBio Integration and the Department of Pathology in the National Institute of Infectious Diseases, Japan, for use of their confocal microscope.

Author Contributions

Conceived and designed the experiments: T. Ando, H. Imamura, T. Wakita, T. Suzuki. Performed the experiments: T. Ando, H. Aizaki. Analyzed the data: T. Ando, H. Imamura, T. Watanabe, T. Wakita, T. Suzuki. Contributed reagents/materials/analysis tools: H. Imamura, R. Suzuki, H. Aizaki. Wrote the paper: T. Ando, T. Suzuki.

References

1. Ranji A, Boris-Lawrie K (2010) RNA helicases: Emerging roles in viral replication and the host innate response. RNA Biol 7: 775–787.
2. Imamura H, Nhat KP, Togawa H, Saito K, Iino R, et al. (2009) Visualization of ATP levels inside single living cells with fluorescence resonance energy transfer-based genetically encoded indicators. Proc Natl Acad Sci U S A 106: 15651–15656.
3. Kato-Yamada Y, Yoshida M (2003) Isolated epsilon subunit of thermophilic F1-ATPase binds ATP. J Biol Chem 278: 36013–36016.
4. Iino R, Murakami T, Iizuka S, Kato-Yamada Y, Suzuki T, et al. (2005) Real-time monitoring of conformational dynamics of the epsilon subunit in F1-ATPase. J Biol Chem 280: 40130–40134.
5. Yagi H, Kajiwara N, Tanaka H, Tsukihara T, Kato-Yamada Y, et al. (2007) Structures of the thermophilic F1-ATPase epsilon subunit suggesting ATP-regulated arm motion of its C-terminal domain in F1. Proc Natl Acad Sci U S A 104: 11233–11238.
6. Bartenschlager R, Sparacio S (2007) Hepatitis C virus molecular clones and their replication capacity in vivo and in cell culture. Virus Res 127: 195–207.
7. Pezacki JP, Singaravelu R, Lyn RK (2010) Host-virus interactions during hepatitis C virus infection: a complex and dynamic molecular biosystem. Mol Biosyst 6: 1131–1142.
8. Suzuki T, Ishii K, Aizaki H, Wakita T (2007) Hepatitis C viral life cycle. Adv Drug Deliv Rev 59: 1200–1212.
9. Cai Z, Liang TJ, Luo G (2004) Effects of Mutations of the Initiation Nucleotides on Hepatitis C Virus RNA Replication in the Cell. J Virol 78: 3633–3643.
10. Moradpour D, Penin F, Rice CM (2007) Replication of hepatitis C virus. Nat Rev Microbiol 5: 453–463.
11. Dumont S, Cheng W, Serebrov V, Beran RK, Tinoco I, Jr., et al. (2006) RNA translocation and unwinding mechanism of HCV NS3 helicase and its coordination by ATP. Nature 439: 105–108.
12. Frick DN (2007) The hepatitis C virus NS3 protein: a model RNA helicase and potential drug target. Curr Issues Mol Biol 9: 1–20.
13. Miyanari Y, Hijikata M, Yamaji M, Hosaka M, Takahashi H, et al. (2003) Hepatitis C virus non-structural proteins in the probable membranous compartment function in viral genome replication. J Biol Chem 278: 50301–50308.
14. Wakita T, Pietschmann T, Kato T, Date T, Miyamoto M, et al. (2005) Production of infectious hepatitis C virus in tissue culture from a cloned viral genome. Nat Med 11: 791–796.
15. Miyamoto M, Kato T, Date T, Mizokami M, Wakita T (2006) Comparison between subgenomic replicons of hepatitis C virus genotypes 2a (JFH-1) and 1b (Con1 NK5.1). Intervirology 49: 37–43.
16. Mankouri J, Tedbury PR, Gretton S, Hughes ME, Griffin SD, et al. (2010) Enhanced hepatitis C virus genome replication and lipid accumulation mediated by inhibition of AMP-activated protein kinase. Proc Natl Acad Sci U S A 107: 11549–11554.
17. Nakashima K, Takeuchi K, Chihara K, Hotta H, Sada K (2011) Inhibition of hepatitis C virus replication through adenosine monophosphate-activated protein kinase-dependent and -independent pathways. Microbiol Immunol 55: 774–782.